

Diversity in the radiation-induced transcriptomic temporal response of mouse brain tissue regions

Karolina Kulis¹, Sarah Baatout², Kevin Tabury², Joanna Polanska^{1*}, Mohammed Abderrafi Benotmane²

¹ Department of Data Science and Engineering, Silesian University of Technology, Gliwice, Poland

² Radiobiology Unit, Institute for Nuclear Medical Application, Belgian Nuclear Research Centre, Belgium

* Corresponding author: joanna.polanska@polsl.pl

ABSTRACT

A number of studies have indicated a potential association between prenatal exposure to radiation and late mental disabilities. This is believed to be due to long-term developmental changes and functional impairment of the central nervous system following radiation exposure during gestation. This study conducted a bioinformatics analysis on transcriptomic profiles from mouse brain tissue prenatally exposed to increasing doses of X-radiation. Gene expression levels were assessed in different brain regions (cortex, hippocampus, cerebellum) and collected at different time points (at 1 and 6 months after birth) for C57BL mice exposed at embryonic day E11 to varying doses of radiation (0, 0.1 and 1 Gy). This study aimed to elucidate the differences in response to radiation between different brain regions at different intervals after birth (1 and 6 months). The data was visualised using a two-dimensional Uniform Manifold Approximation and Projection (UMAP) projection, and the influence of the factors was investigated using analysis of variance (ANOVA). It was observed that gene expression was influenced by each factor (tissue, time, and dose), although to varying degrees. The gene expression trend within doses was compared for each tissue, as well as the significant pathways between tissues at different time intervals. Furthermore, in addition to radiation-responsive pathways, Cytoscape's functional and network analyses revealed changes in various pathways related to cognition, which is consistent with previously published data [1] [2] [3], indicating late behavioural changes in animals prenatally exposed to radiation

KEYWORDS

Radiation, brain, mouse, microarray, bioinformatics,

INTRODUCTION

Epidemiological data from in utero exposed Hiroshima and Nagasaki A-bomb survivors indicates that prenatal irradiation may severely compromise normal embryonic development, leading to a variety of anatomical, physiological and mental defects. The assessment of radiation exposure can vary for different organisms and cell types involved in radiobiology experiments. Advances have been made in animal models, such as rodents, to explore the effects of radiation on the unborn child. These models have been used to reproduce these effects in order to better understand the underlying cellular and molecular mechanisms. Most research agrees on the idea that the brain is sensitive to radiation at the prenatal or childhood stage. This is presumably due to incomplete developmental processes. A number of authors have reported on the effects of radiation on learning and memory in various types of mazes, including [1], [2], [3], [7], [8], [9], [10]. Despite its therapeutic benefit, radiation therapy is associated with a number of adverse effects, including cognitive and emotional dysfunctions and changes in neuroanatomical structures, particularly in young patients [11], [12]. It is therefore of great importance to assess the impact of radiation on living organisms and to identify markers that allow for the assessment of the absorbed dose. This article presents a bioinformatics analysis of the potential effects of radiation exposure during early gestation on gene expression in adulthood. The study aims to investigate differences in response to irradiation between brain regions by examining whether there are robust, tissue-, time-, and dose-independent biomarkers of irradiation and comparing gene expression values for different doses. The objective of this study is to investigate the differences in response to irradiation between brain regions. In addition, the study aims to identify robust, tissue-, time-, and dose-independent biomarkers of irradiation and to compare gene expression levels for different doses.

MATERIAL AND METHODS

Animals and irradiation

All animal experiments were performed in accordance with the European Communities Council Directive (2010/63/EU) and approved by the local ethical SCK•CEN (Brainres) or SCK•CEN/VITO (ref. 02–012 and 11-005), University of Antwerp and KU Leuven committees. C57Bl/6J were purchased from Janvier (Bio Services, Uden, The Netherlands) or from Charles River Breeding Laboratories (Leiden, The Netherlands). Animals were housed under standard laboratory conditions (12-h light/dark cycle) and food and water were available *ad libitum*. Female mice were coupled during a 2-h time period in the morning, at the start of the light phase, in order to ensure synchronous timing of embryonic development. Subsequently, dams were whole-body irradiated at E11 (0.10 or 1.00 Gy) at a dose rate of 0.35 Gy min⁻¹ using a Pantak RX tube operating at 250 kV and 15 mA (1-mm Cu-filtered X-rays). The calibration of this X-ray tube was performed using an ionisation chamber. For all irradiation procedures, mice were placed in a plexiglass pie-shaped box, in which their movement was restricted. Subsequently, the plexiglass box containing the animals was transported to the irradiation facility and placed within the radiation field, ensuring an equal dose distribution to all mice. After the irradiation, mice were placed back (returned) to their home cage. Control mice were sham-irradiated, i.e. they underwent all procedures similar to irradiated animals but were not placed within the radiation field.

Microarray-based transcriptomic profile measurement

Total RNA was extracted from flash-frozen adult brain tissues (Cortex, hippocampus and cerebellum) at 1 or 6 months after birth using the AllPrep DNA/RNA/Protein Mini Kit (Qiagen, Hilden, Germany) and quality-controlled using the 2100 BioAnalyzer (Agilent, Santa Clara, CA, US). Only samples with an RNA integrity number >8 were used for hybridisation onto Affymetrix Mouse Gene 2.0 ST arrays (Affymetrix, Santa Clara, CA, US) as per the manufacturer's recommendations. CEL files were uploaded for subsequent bioinformatics analyses. Data normalisation was performed using a customised Robust Multi-array Average algorithm (background correction for entire probe sequence, quantile normalisation, log₂ transformation of intensity signals).

Statistical analysis

Statistical analysis was performed using NumPy, Pandas, Scikit-learn, Statsmodels, and Matplotlib, in Python version 3.10. Descriptive statistics, including minimum and maximum values, mean, median, standard deviation, lower and upper quartiles, and interquartile range, were calculated for each variable and dose/timepoint, along with their corresponding 95% confidence intervals. The internal data structure was visualised and investigated using the UMAP [13] transformation. To achieve this, the PCA high-dimensionality reduction technique was used to select the first components that explain 95% of the total variance in the dataset. Subsequently, the data was transformed using the 2D UMAP transformation with the new PCA-based set of features and Euclidean similarity measure. Outliers were checked using Dixon's Q test. A three-way analysis of variance (ANOVA) test was performed to identify differentially expressed genes, with tissue, time, and dose as independent variables. The general effect size was estimated as eta squared [14] and modified Glass delta estimates supported post hoc pairwise comparisons. The analyses were summarised using Venn diagrams. The further study investigated the dose trend for genes that did not exhibit significant interactions between factors across various brain regions and time intervals following exposure to irradiation.

Functional analysis

Functional analysis using Gene Set Enrichment Analysis (GSEA) [15] [16] was performed to identify radiation-enriched signalling pathways. It was done mostly in R programming language version 4.3.1 and Bioconductor's *fgsea* package. All genes from the original dataset were used and ranked according to the effect size value of the dose factor [14]. MSigDB database was used to gather only the gene sets related to irradiation and brain development. Additionally, we applied a filter to the database of gene sets for mice species using a set of keywords to be found in the pathway descriptions. The keywords we used were *radiation*, *irradiation*, *cognitive function*, *brain development*, *neurological response*, *neurogenesis*, *memory*, *cognition*, *behaviour*, and *learning*. The signalling pathway filtration procedure resulted in a selection of 860 gene sets that were considered in our functional analysis. The gene sets resulting from the GSEA were carefully curated to ensure that only pathways relevant to the project's aim were included. Pathways that were not associated with neurological functions were excluded. For further details, please refer to the supplementary materials (Table S3-S8, Figure S1-S6). The relationship networks between gene sets with an enrichment p-value < 0.05, which were considered significantly enriched, were jointly analyzed using Cytoscape software after calculating the similarity coefficient.

RESULTS

Gene expression levels of 27,352 transcripts, assessed in different brain regions (cortex, hippocampus, cerebellum) and collected at different time points (at 1 and 6 months after birth) of C57bl mice exposed during gestation at embryonic day E11 to different doses of radiation (0, 0.1 Gy and 1 Gy) constituted the data.

PCA technique, with choosing the components explaining 95% of the total variance in the dataset, reduced the dimension from 27,352 to 53. The 2D UMAP transformation was then applied, resulting in a plot shown in Figure 1. To make the visualisation clearer and more legible, the differentiating factors were distinguished as follows: different doses were differentiated on the plot with colour, time with size and tissue with shape. One sample was tested positive for being an outlier using Dixon's Q test and removed from further analysis.

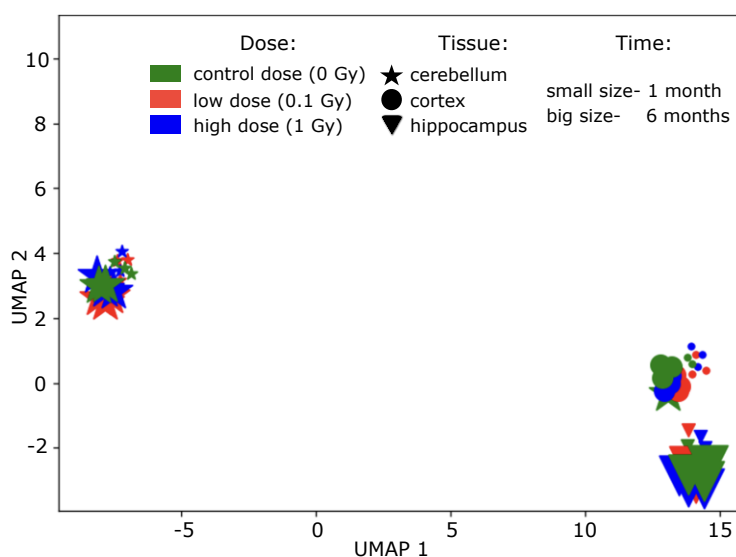


Figure 1. Data visualised- UMAP transformation with differentiation by factors.

Three-way Analysis of Variance (ANOVA), where the independent variables were tissue, time and dose, while the response variable was the gene expression, was performed and supported by the eta-squared effect size measures. The genes with at least a large effect size for all factors (main effects separately and interactions between them) were summarised in the Venn diagram (see Figure 2).

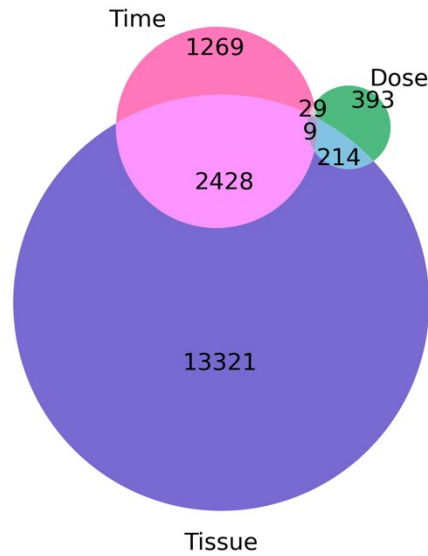


Figure 2. Venn diagram of large effects (numbers within each circle correspond to the number of genes fulfilling the selection criterion)

Performing ANOVA has proved that each factor (tissue, time and dose) has influenced gene expression, although each to a different degree. The tissue factor differentiated the most and time the least, which was already noticeable after applying UMAP transformation to the data. 13,321 transcripts were tissue-, 1,269 time-, and 393 were dose-dependent only with at least a large effect size. 29 transcripts were time- and dose-dependent, 214 dose- and tissue-dependent and 2428 time- and tissue-dependent. 9 genes had a large effect value for all factors.

The gene expression time series were investigated to check how gene expression reacted after the irradiation. From the 393 dose-dependent genes, the ones that had no significant interactions between the differentiating factors were considered (see supplementary materials). To demonstrate the impact of the interaction on the gene expression response, Figure 3A presents an example of a gene with inter-factor interactions. Figure 3B shows a case where the interactions are not significant – tissue-specific time responses seem to be similar.

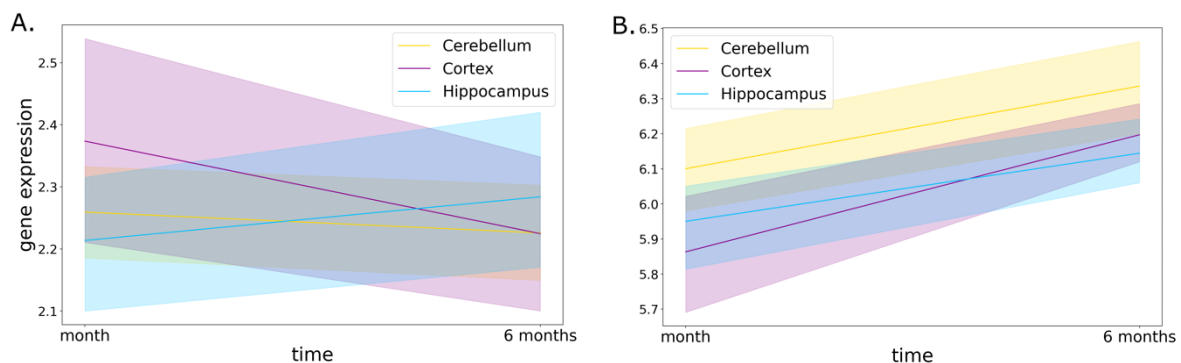


Figure 3. A. Interaction plot of a gene with significant interactions between factors (left panel) tissue dependent different time responses B. Interaction plot of a gene with no significant interactions between factors (right panel). The solid lines represent the approximated time response for different tissue samples, while the colour-coded shadowed area visualises their 95% confidence intervals.

A similar trend analysis was performed for the dose series (for the 393 genes) within various brain regions and in different time intervals after the exposure of irradiation. The constant increase of gene expression (control dose < low dose < high dose) or constant decrease in dose (control dose > low dose > high dose), independently of time point, is an example of dose dependency. The examples of boxplots presenting such a behaviour can be seen in Figure 4 (panels A and B), where the yellow line presents the median of gene expression for different doses. At one month after exposure to irradiation, a constant increase in dose was observed in 52 genes for the cerebellum, 54 genes for the cortex and 50 genes for the hippocampus, while the constant decrease was present in 41 genes for the cerebellum, 46 genes for the cortex and 49 genes for the hippocampus (see Table 1). After six months of irradiation, the increasing trend was observed in 52 genes for the cerebellum tissue, 51 genes for the cortex and 72 genes for the hippocampus, while the decreasing trend was present in 57 genes for the cerebellum, 53 genes for the cortex and 44 genes for the hippocampus (see Table 2). The full list of genes [17] obtained in each group can be studied in the supplementary materials (Tables S1 and S2). A literature review of the genes [18] obtained in each group was performed to identify the genes that are functionally most related to the effect of radiation on neurological and cognitive functions in different brain tissues. The ascending trend in the tissues was observed among others in *Tti2* (encodes a regulator of the DNA damage response; the protein is a component of the Triple T complex (TTT), which also includes telomere length regulation protein and TELO2 interacting protein 1) for cerebellum after one month of irradiation and for hippocampus after both one and six months after the exposure. In the cerebellum, this trend was also present in the *Tcf4* gene (encodes transcription factor 4, a basic helix-loop-helix transcription factor) independently of the time factor. After six months of irradiation, the same pattern in dose was observed in *Ecr4* (Esophageal Cancer Related Gene 4 Protein enables neuropeptide hormone activity; involved in neuropeptide signalling pathway; positive regulation of hormone secretion; and vasopressin secretion) for cerebellum and cortex. One month after the exposure, both *Gsc* (Goosecoid Homeobox, connected with nervous system development) and *Txlna* (Taxilin Alpha, predicted to enable syntaxin binding activity) presented an increasing trend in dose for the hippocampus but decreased for the cerebellum. *Gsc* also showed a constant decrease in gene expression after six months of irradiation for the cortex. *Tcof1* (Treacle Ribosome Biogenesis Factor 1, encodes a nucleolar protein with a LIS1 homology domain; required for neural crest specification) gene was present in every group independently of time and tissue, besides cerebellum at one month after the exposure. The Venn diagram in Figures 5A and 5B presents the observed similarity in dose trends.

Another dose-response pattern that has been often observed showed either an increase of gene expression for low dose compared to the control dose and a decrease for high dose compared to the control dose, or the opposite - a decrease of gene expression for low dose compared to control dose and increase for high dose compared to control dose (Figure 4, panels C and D). Such a pattern, which we named Ω -shaped and U-shaped, with different responses to corresponding doses, was also observed in each tissue (see Figure 5C and 5D). At one month after the exposure to irradiation, the Ω -shaped pattern was observed in 63 genes for the cerebellum, 50 genes for the cortex and 44 genes for the hippocampus, while the U-shaped pattern was present in 41 genes for the cerebellum, 58 genes for the cortex and 61 genes for the hippocampus (see Table 1). However, after six months, the Ω -shaped pattern was present in 36 genes for both the cerebellum and cortex and 40 genes for the hippocampus, while the U-shaped pattern was observed in 35 genes for the cerebellum, 62 genes for the cortex and 56 genes for the hippocampus (see Table 2). The full list of genes for each group can be seen in Tables S1 and S2. Repeatedly, the literature on the resulting genes was reviewed to find those associated with radiation-induced neurological functions. After one month of irradiation, the

Ω -shaped pattern was present in *Ecr4* and *Vmn1r43* (Vomeronasal type-1 receptor 43; putative pheromone receptor implicated in the regulation of social and reproductive behaviour) for both cortex and hippocampus, but *Vmn1r43* also for cerebellum. *Chrd11* (Chordin Like 1, alters the fate commitment of neural stem cells from gliogenesis to neurogenesis) presented an example of such a trend in the cortex independently of time. After one month of irradiation, a few more genes were also presenting the Ω -shaped pattern, such as *Npy6r* (encodes Neuropeptide Y Receptor Y6, predicted to be involved in neuropeptide signalling pathway) for the cerebellum, *Txlna* and *Gsc* for cortex and *Tcf4* for the hippocampus. That trend was also visible after six months of the exposure in *Gsc* for cerebellum, *Hsd17b10* (encoding 3-hydroxyacyl-CoA dehydrogenase type II, a member of the short-chain dehydrogenase/reductase superfamily) for cortex and *Txlna* for hippocampus. The U-shaped pattern after one month of irradiation was present in *Ecr4* for the cerebellum, *Tcf4* and *Tti2* for the cortex and in *Hsd17b10* for both the cortex and hippocampus. After six months of exposure to irradiation, that trend in dose was observed in *Tti2* for the cerebellum, *Ecr4* and *Gsc* for the hippocampus, in *Npy6r* for both cerebellum and hippocampus and in *Txlna* for the cerebellum and cortex.

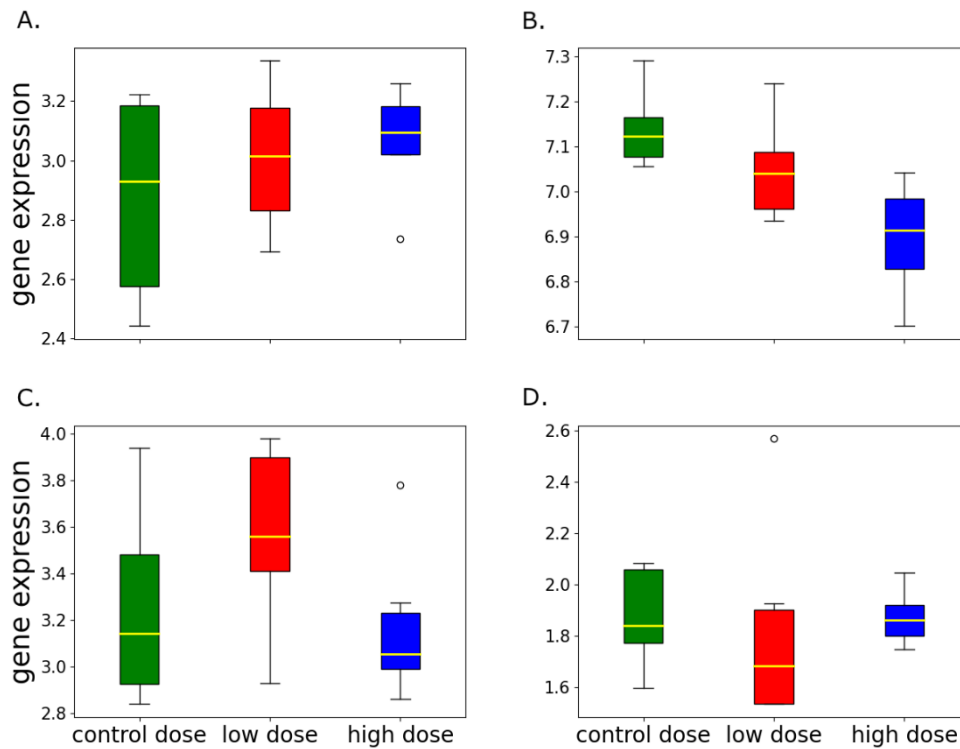


Figure 4. Examples of different patterns in dose-response: additive increase of gene expression in the dose (panel A), additive decrease of gene expression within the dose (panel B), Ω -shaped (panel C) and U-shaped (panel D) dose responses.

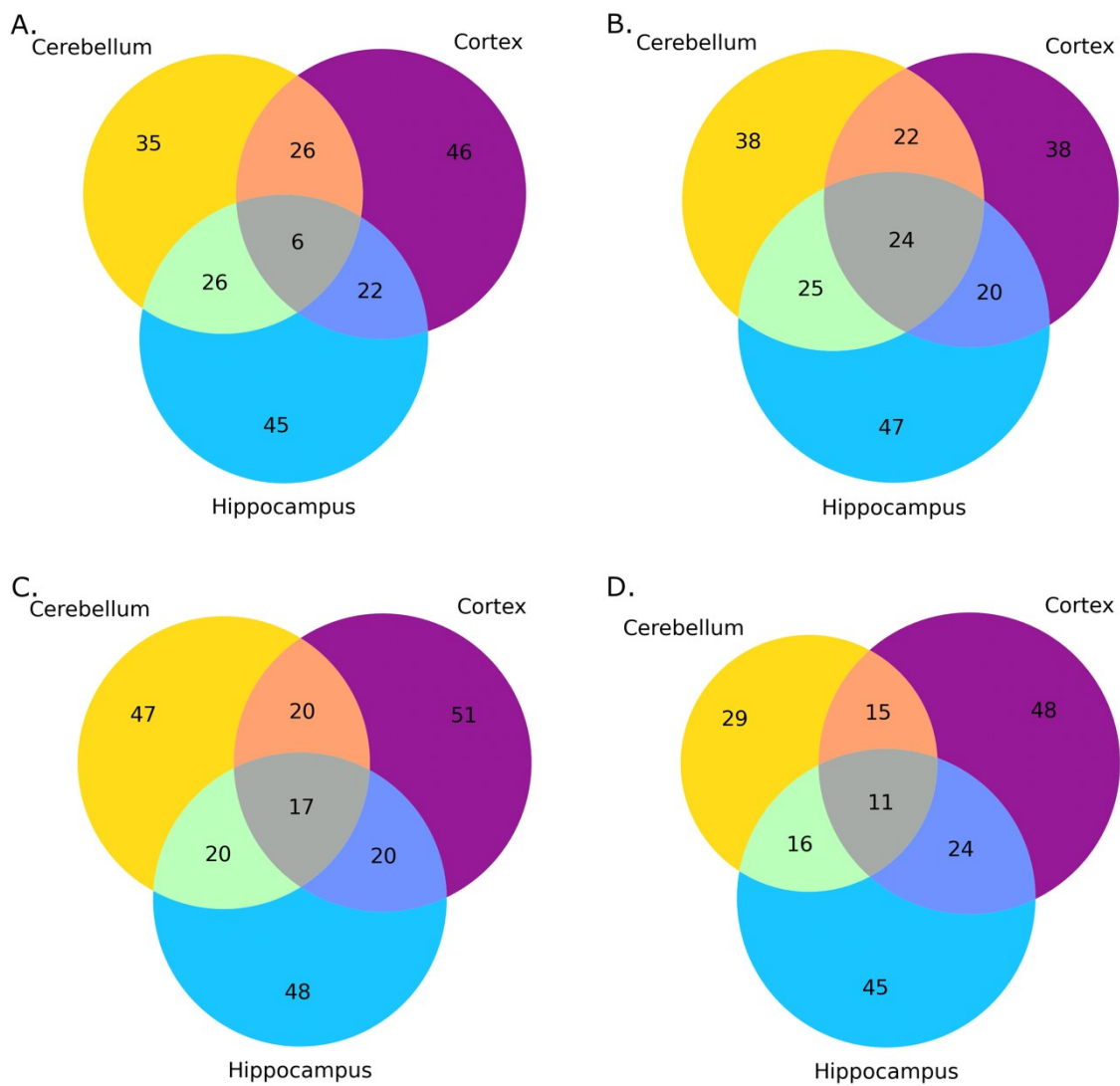


Figure 5. Venn diagram of the number of genes in which either constant increase or decrease of the gene expression in dose has been observed after one month of irradiation (A.) and six months after irradiation (B.) or U-shape increase or decrease after one month of irradiation (C.) and six months after irradiation (D.).

Table 1. A number of genes in the studied brain tissues showing certain dose trends after one month of irradiation.

	Additive increase	Additive decrease	U-shaped	Ω-shaped
cerebellum	52	41	41	63
cortex	54	46	58	50
hippocampus	50	49	61	44

Table 2. A number of genes in the studied brain tissues showing certain dose trends after six months of irradiation.

	Additive increase	Additive decrease	U-shaped	Ω-shaped
cerebellum	52	57	35	36
cortex	51	53	62	36
hippocampus	72	44	56	40

The study employed Gene Set Enrichment Analysis (GSEA) to conduct functional analysis six times for each time/tissue endpoint, which allowed comparison of the dose-dependent enrichment of gene sets with keywords related to the study's objective and to observe tissue differentiation in mice of different ages. A one-way ANOVA was performed for each specific brain tissue sample during the selected time interval, with dose as the independent factor and gene expression as the response variable. Gene sets specific to radiation exposure were identified as significant through GSEA and manual curation in tissues at one month (Figure 6A) and six months (Figure 6B) after exposure.

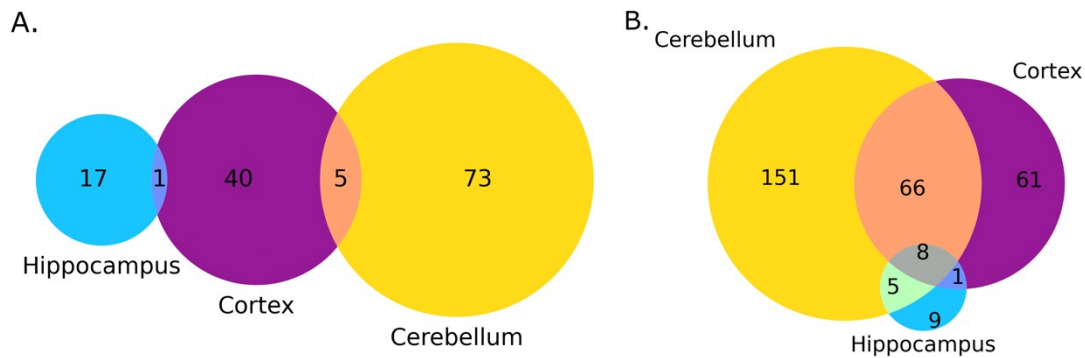


Figure 6. A. Comparison of chosen significant gene sets after GSEA with radiation-specific gene sets, between tissues after one month of irradiation. B. Comparison of significant gene sets after GSEA with radiation-specific gene sets between tissues after six months of irradiation.

The resulting pathways for every tissue and time interval after the irradiation can be studied in Tables S3-S8.

For each group that combines a specific tissue with a particular time period, the similarity coefficient was calculated for every pair of pathways in the significantly enriched gene sets. The similarity coefficient was determined as the fraction of genes shared by both pathways to the total number of unique genes present in those pathways. This approach allows for a comprehensive analysis of the pathways and their shared genes. The pathways were visualised using Cytoscape software. Nodes were used to represent the pathways and were connected by edges whose thickness was adjusted based on the similarity coefficient value. An edge threshold was applied to eliminate connections between gene sets that had no genes in common or had a very small similarity coefficient. This helped to improve the clarity and legibility of the visualisations. For all the tested tissues after 6 months of irradiation, the similarity coefficient threshold was set to 0.04. However, after 1 month of irradiation, the threshold for the cerebellum and cortex was set to 0.02, while for the hippocampus, it was set to 0.01 due to the limited number of significant pathways associated with the irradiation term. The networks for each tissue examined after 1 month of irradiation are presented in the left column of Figure 7, and after 6 months of irradiation, they are presented in the right column. Clusters related to changes in behaviour or the radiation response are visible in every network, although they are most prominent and dense in tissues 6 months after irradiation.

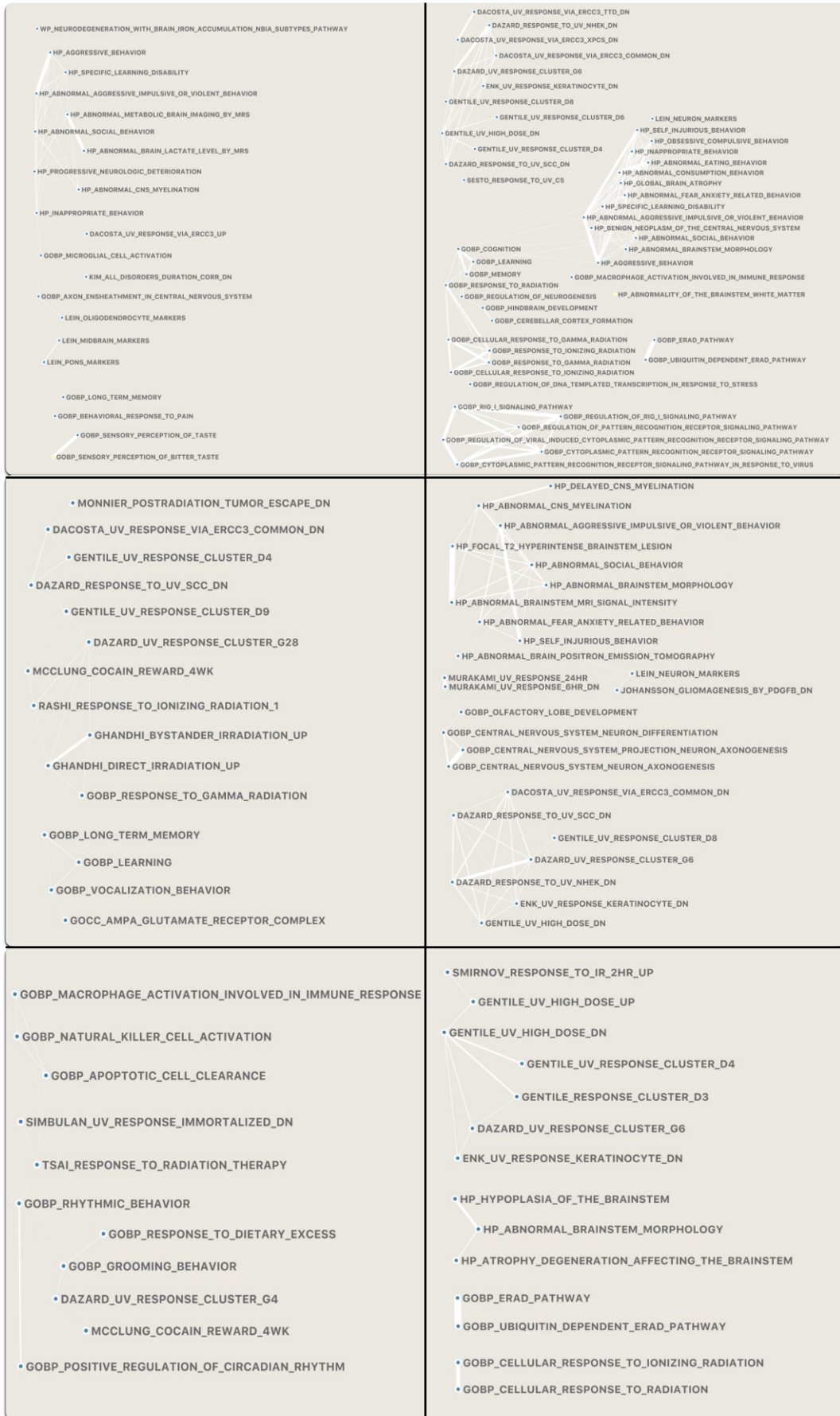


Figure 7. Network presenting pathway connections for cerebellum (first row), cortex (second row) and hippocampus (third row) after one month of irradiation (left column) and six months after the irradiation (right column).

DISCUSSION

Since its discovery, ionising radiation has proven to be a double-edged sword. Its use in the medical field has meant a tremendous step forward in health care. However, it must be utilised with caution since exposure to radiation might as well provoke serious health consequences. In the first instance, the atomic bomb survivor studies have been indispensable in the evaluation of radiation-induced sequelae because of the use of large cohorts and a long-term follow-up. In these studies, radiation exposure was shown to induce cancer and leukaemia in a linear dose-dependent manner, although evidence for this becomes more ambiguous around doses below 100 mGy. Non-cancer effects, including cardiovascular diseases, cataracts, and postnatal/adult radiation-induced cognitive dysfunction, were also uncovered in epidemiological research but were believed to only arise after high-dose exposure. Recently, evidence accumulated that these non-cancer effects might as well be caused by doses around and below 0.5 Gy. As a general standard, pregnant women are better protected against ionising radiation than the general population because of the known adverse outcome for the unborn child, which has a high sensitivity to radiation-induced cancer. Importantly, besides cancer, prenatal irradiation can perturb brain development and cause neurological deficits, which were also demonstrated and evidenced for the first time by the atomic bomb survivor studies. On the other hand, we convincingly have shown in previous work in utero exposure to radiation-induced effects at low (0.1 Gy) and high (1.0 Gy) doses. In the short-term, 1.0 Gy irradiation (to a lesser extent 0.1 Gy) at E11 significantly induced DNA damage, cell cycle arrest and apoptosis, as well as an altered distribution of recently differentiated cells [1], [2], [3]. Mice exposed to 1.0 Gy (to a lesser extent 0.1 Gy) were defective in emotional responding and spatio-cognitive performance at a young adult age.

This paper attempts to illustrate the transcriptomic changes at 1 month and 6 months after birth in the brains of animals prenatally exposed to radiation. For that, combining the work of bioinformaticians and biologists was imperative. Advanced bioinformatics tools have been used for functional analysis. Still, the opinion and vision based on a biologist's background are highly appreciated in relation to pathways to answer the question in line with the project objectives. This ensures that the results are coherent and that the progress of the project can move in the desired direction.

The statistical analysis aimed to uncover the gene profile after irradiation in different brain regions at different time intervals after exposure to irradiation. The data was first visualised using dimensionality reduction techniques, which helped to provide an overview of the differentiation between factors. An analysis of variance (ANOVA) statistical test was applied to every gene to detect differences between the means of the experimental groups. The genes with at least a large effect size value only for the dose factor were taken into further analysis that had no interactions between the three differentiating factors. Various trends within doses were found and described.

Consecutively, functional analysis was performed, which sought to provide biological context to the groups that combined selected tissues with specific time intervals. A Gene Set Enrichment Analysis (GSEA) was performed for each group using gene sets related to irradiation to enrich the pathways. Statistically significant pathways were then manually curated by a biologist to select only those that fit the purpose of the study. Their networks with connections between pathways according to the similarity coefficient were visualised for each group. The formed clusters were then analysed, and each group that combined a certain tissue with a specific period of time was compared, to see how the tissues vary at different ages of

mice. Of note, irradiation-induced apoptosis during gestation is considered protective to the developing embryo to eliminate damaged cells in a p53-dependent way [19], which might hamper further normal development. Therefore, we analysed the gene expression profiles in postnatal animals at 1 month and 6 months to establish a causal link between short- and long-term prenatal radiation effects. The identified GSEA and network pathways of the analysed brain regions (hippocampus, cortex and cerebellum) provided valuable information on brain behaviour-related pathways which are fully in line with previously performed behavioural testing and magnetic resonance imaging data [1], [2], [3]. For instance, in the cerebellum at 1 month, the most significant pathways are related to aggressive behaviour, abnormal social behaviour, learning disability, long-term memory, CNS myelination, oligodendrocyte and midbrain markers. At 6 months, these pathways appear less remarkable but persist with less significance for learning, aggressive behaviour, inappropriate behaviour and myelination. In the cortex, at 1 month, we mostly observe pathways involved in radiation (UV or Gamma) response, learning, long-term memory, and neuron development. In the 6 months, more significance is observed for pathways such as abnormal social behaviour, CNS myelination, neuron markers, aggressive, impulsive behaviour, brainstem markers, anxiety, axonogenesis and neuron differentiation. On the contrary, in the hippocampus, very few behaviour-related pathways are significant; at 1 month, we observe grooming behaviour, rhythmic behaviour and positive regulation of circadian rhythm; at 6 months, mainly pathways involved in hypoplasia and degeneration of the brainstem and abnormal brainstem development and morphology, indicating a defect in brain connections and brain communication. In all, we believe that the performed transcriptomic functional analysis strongly supports our previous observations by [1], [2], [3]. The identified pathways can be considered a valid biomarker for prenatal radiation-induced late cognitive impairment.

CONCLUSIONS

It is extremely important to assess the impact of radiation on living organisms. Raising awareness of radiation defects in the developing brain is of utmost importance. This paper aims to illustrate the transcriptomic changes in the brain of animals prenatally exposed to radiation at 1 and 6 months after birth. Communication was effectively maintained between the bioinformatician and the biologist throughout the project, and frequent discussions were held to ensure progress in the right direction. It is recommended that both statistical and functional analysis be carried out to understand the results fully. The statistical analysis suggests that tissue plays a primary role in distinguishing gene expression, and each brain region exhibits varying degrees of sensitivity. The gene profiles revealed distinct responses to irradiation in different tissues. Detailed descriptions of the statistically significant pathway networks were provided for each tissue at various time intervals after radiation. The pathways that were found to be most activated appear to be related to behavioural changes and the response to irradiation. The results are satisfactory and strongly support previous observations. Therefore, the identified pathways could be considered a valid biomarker for prenatal radiation-induced late cognitive impairment.

ACKNOWLEDGEMENT

Project was partially financed by Belgian Royal Decree 24.06.2021, Project ID: 21. Most of the transcriptomic data discussed in this paper were obtained within the FP7 EU CEREBRAD project (GA 295552)

This work has been partially supported by the ENEN2plus project (HORIZON-EURATOM-2021-NRT-01-13 101061677) funded by the European Union.

BIBLIOGRAPHY

- [1] Verreet, T., Verslegers, M., Quintens, R., Baatout, S., and Benotmane, M. A., 2016, “Current Evidence for Developmental, Structural, and Functional Brain Defects Following Prenatal Radiation Exposure,” *Neural Plast.*, **2016**.
- [2] Verreet, T., Quintens, R., Van Dam, D., Verslegers, M., Tanori, M., Casciati, A., Neefs, M., Leysen, L., Michaux, A., Janssen, A., D’Agostino, E., Velde, G. Vande, Baatout, S., Moons, L., Pazzaglia, S., Saran, A., Himmelreich, U., De Deyn, P. P., and Benotmane, M. A., 2015, “A Multidisciplinary Approach Unravels Early and Persistent Effects of X-Ray Exposure at the Onset of Prenatal Neurogenesis,” *J. Neurodev. Disord.*, **7**(1), pp. 1–21.
- [3] Verreet, T., Rangarajan, J. R., Quintens, R., Verslegers, M., Lo, A. C., Govaerts, K., Neefs, M., Leysen, L., Baatout, S., Maes, F., Himmelreich, U., D’Hooge, R., Moons, L., and Benotmane, M. A., 2016, “Persistent Impact of in Utero Irradiation on Mouse Brain Structure and Function Characterized by MR Imaging and Behavioral Analysis,” *Front. Behav. Neurosci.*, **10**(MAY), pp. 1–18.
- [4] Russell, D. W., Kahn, J. H., Spoth, R., & Altmaier, E. M., 1998, “Analyzing Data from Experimental Studies: A Latent Variable Structural Equation Modeling Approach,” *J. Couns. Psychol.*
- [5] Belli, M., and Indovina, L., 2020, “The Response of Living Organisms to Low Radiation Environment and Its Implications in Radiation Protection,” *Front. Public Heal.*, **8**(December), pp. 1–15.
- [6] Tapio, D. H. S., 2016, “Exposure of Ionizing Radiation on the Mammalian Brain: Epidemiological Evidence, Pathological and Molecular Effects and Prevention Strategies,” *Mutat. Res.*
- [7] M. Hossain, P. U. D., 2001, “Effect of Irradiation at the Early Foetal Stage on Adult Brain Function of Mouse: Learning and Memory,” *Int. J. Radiat. Biol.*
- [8] Andrzej Sienkiewicz, Ana Maria da Costa Ferreira, Birgit Danner, C. P. S., 1999, “Dielectric Resonator-Based Flow and Stopped-Flow EPR with Rapid Field Scanning: A Methodology for Increasing Kinetic Information,” *J. Magn. Reson.*
- [9] Andrzej Sienkiewicz, Kunbin Qu, and C. P. S., 1994, “Dielectric Resonatorbased Stoppedflow Electron Paramagnetic Resonance,” *Rev. Sci. Instrum.*
- [10] Surendran HP, Narmadha MP, Kalavagunta S, Sasidharan A, D. D., 2022, “Preservation of Cognitive Function after Brain Irradiation,” *J. Oncol. Pharm. Pract.*
- [11] Marazziti, D., Baroni, S., Catena-Dell’Osso, M., Schiavi, E., Ceresoli, D., Conversano, C., Dell’Osso, L., and Picano, E., 2012, “Cognitive, Psychological and Psychiatric Effects of Ionizing Radiation Exposure,” *Curr. Med. Chem.*, **19**(12), pp. 1864–1869.
- [12] Marazziti, D., Piccinni, A., Mucci, F., Baroni, S., Loganovsky, K., and Loganovskaja, T., 2016, “Ionizing Radiation: Brain Effects and Related Neuropsychiatric Manifestations,” *Probl. Radiatsii noi Medytsyny ta Radiobiologii*, **2016**(21), pp. 64–90.
- [13] McInnes, L., Healy, J., and Melville, J., 2018, “UMAP: Uniform Manifold Approximation and Projection for Dimension Reduction.”
- [14] Cohen, J., 1988, *Statistical Power Analysis for the Behavioral Sciences*.
- [15] Subramanian, A., Tamayo, P., Mootha, V. K., Mukherjee, S., Ebert, B. L., Gillette, M. A., Paulovich, A., Pomeroy, S. L., Golub, T. R., Lander, E. S., and Mesirov, J. P., 2005, “Gene Set Enrichment Analysis: A Knowledge-Based Approach for Interpreting

- Genome-Wide Expression Profiles,” *Proc. Natl. Acad. Sci. U. S. A.*, **102**(43), pp. 15545–15550.
- [16] Mootha, V., Lindgren, C., Eriksson, K. et al, 2003, “PGC-1 α -Responsive Genes Involved in Oxidative Phosphorylation Are Coordinately Downregulated in Human Diabetes,” *Nat Genet.*
- [17] Koopmans, F., van Nierop, P., Andres-Alonso, M., Byrnes, A., Cijssouw, T., Coba, M. P., Cornelisse, L. N., Farrell, R. J., Goldschmidt, H. L., Howrigan, D. P., Hussain, N. K., Imig, C., de Jong, A. P. H., Jung, H., Kohansalnodehi, M., Kramarz, B., Lipstein, N., Lovering, R. C., MacGillavry, H., Mariano, V., Mi, H., Ninov, M., Osumi-Sutherland, D., Pielot, R., Smalla, K.-H., Tang, H., Tashman, K., Toonen, R. F. G., Verpelli, C., Reig-Viader, R., Watanabe, K., van Weering, J., Achsel, T., Ashrafi, G., Asi, N., Brown, T. C., De Camilli, P., Feuermann, M., Foulger, R. E., Gaudet, P., Joglekar, A., Kanellopoulos, A., Malenka, R., Nicoll, R. A., Pulido, C., de Juan-Sanz, J., Sheng, M., Südhof, T. C., Tilgner, H. U., Bagni, C., Bayés, À., Biederer, T., Brose, N., Chua, J. J. E., Dieterich, D. C., Gundelfinger, E. D., Hoogenraad, C., Huganir, R. L., Jahn, R., Kaeser, P. S., Kim, E., Kreutz, M. R., McPherson, P. S., Neale, B. M., O’Connor, V., Posthuma, D., Ryan, T. A., Sala, C., Feng, G., Hyman, S. E., Thomas, P. D., Smit, A. B., and Verhage, M., 2019, “SynGO: An Evidence-Based, Expert-Curated Knowledge Base for the Synapse.,” *Neuron*, **103**(2), pp. 217-234.e4.
- [18] “GeneCards – the Human Gene Database” [Online]. Available: <https://www.genecards.org>.
- [19] Quintens, R., Verreet, T., Janssen, A., Neefs, M., Leysen, L., Michaux, A., Verslegers, M., Samari, N., Pani, G., Verheyde, J., Baatout, S., and Benotmane, M. A., 2015, “Identification of Novel Radiation-Induced P53-Dependent Transcripts Extensively Regulated during Mouse Brain Development,” *Biol. Open*, **4**(3), pp. 331–344.

Diversity in the radiation-induced transcriptomic temporal response of mouse brain tissue regions

Karolina Kulis, Sarah Baatout, Kevin Tabury, Joanna Polanska, Mohammed Abderrafi Benotmane

SUPPLEMENTARY MATERIALS



Figure S1. Dotplot presenting chosen significantly enriched pathways with p value < 0.05, for one month after irradiation for cerebellum

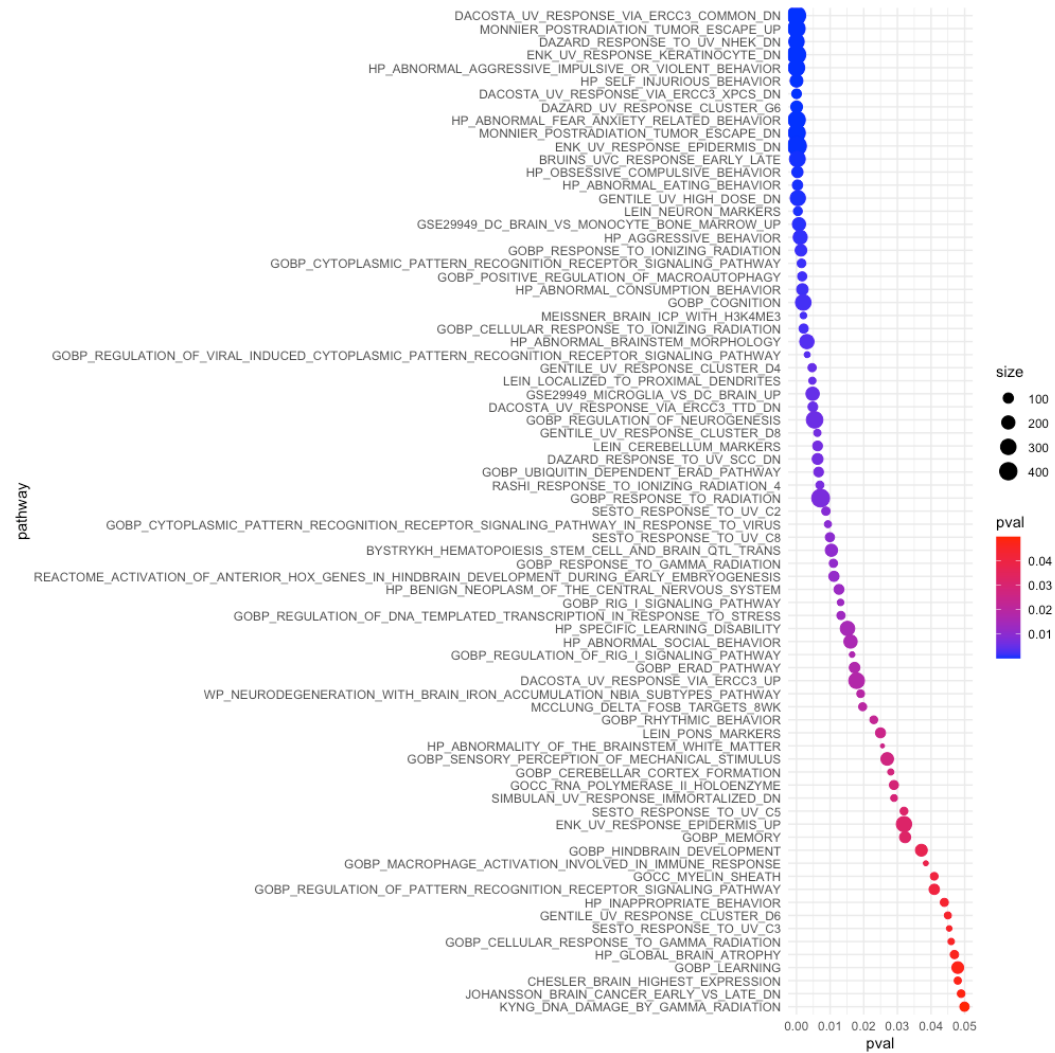


Figure S2. Dotplot presenting chosen significantly enriched pathways with p value < 0.05, for six months after irradiation for cerebellum

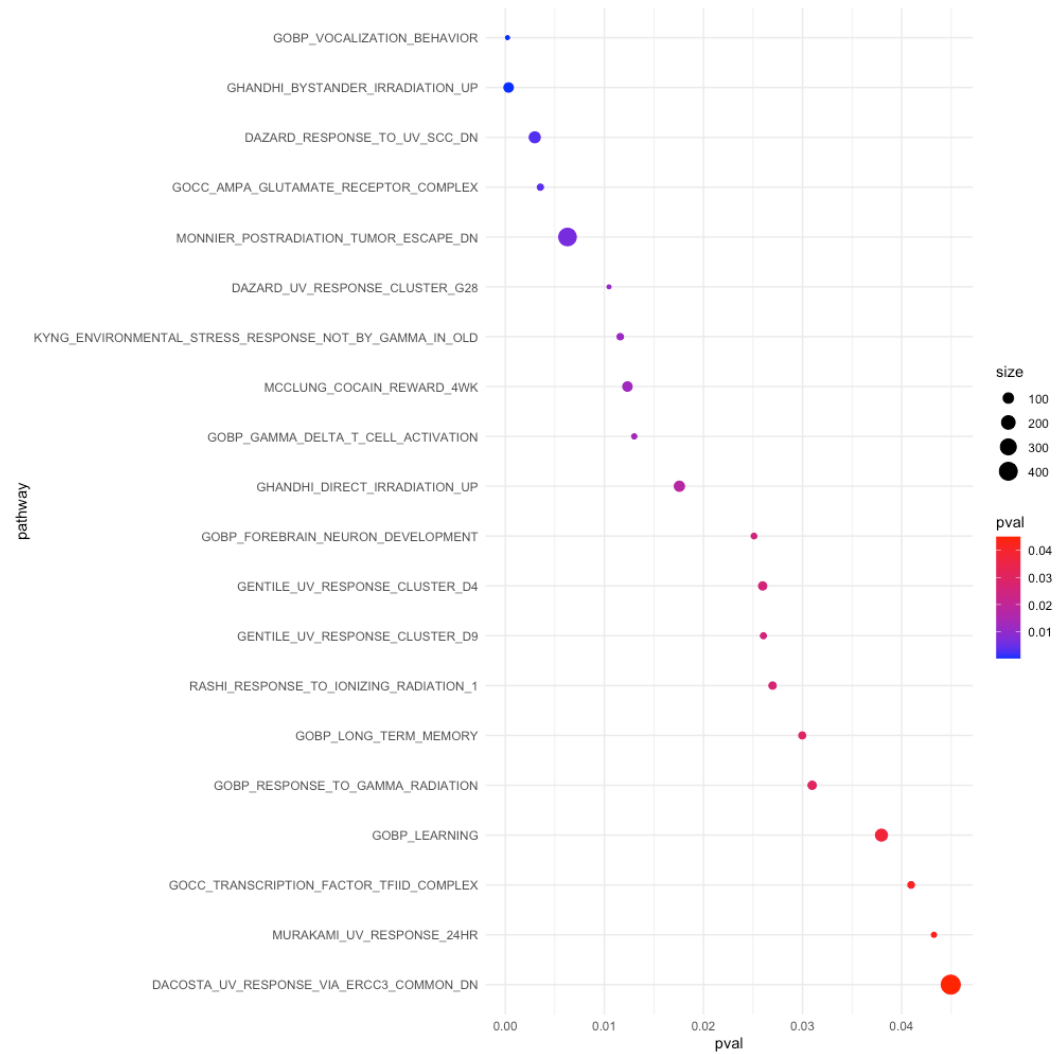


Figure S3. Dotplot presenting chosen significantly enriched pathways with p value < 0.05 , for one month after irradiation for cortex



Figure S4. Dotplot presenting chosen significantly enriched pathways with p value < 0.05 , for six months after irradiation for cortex

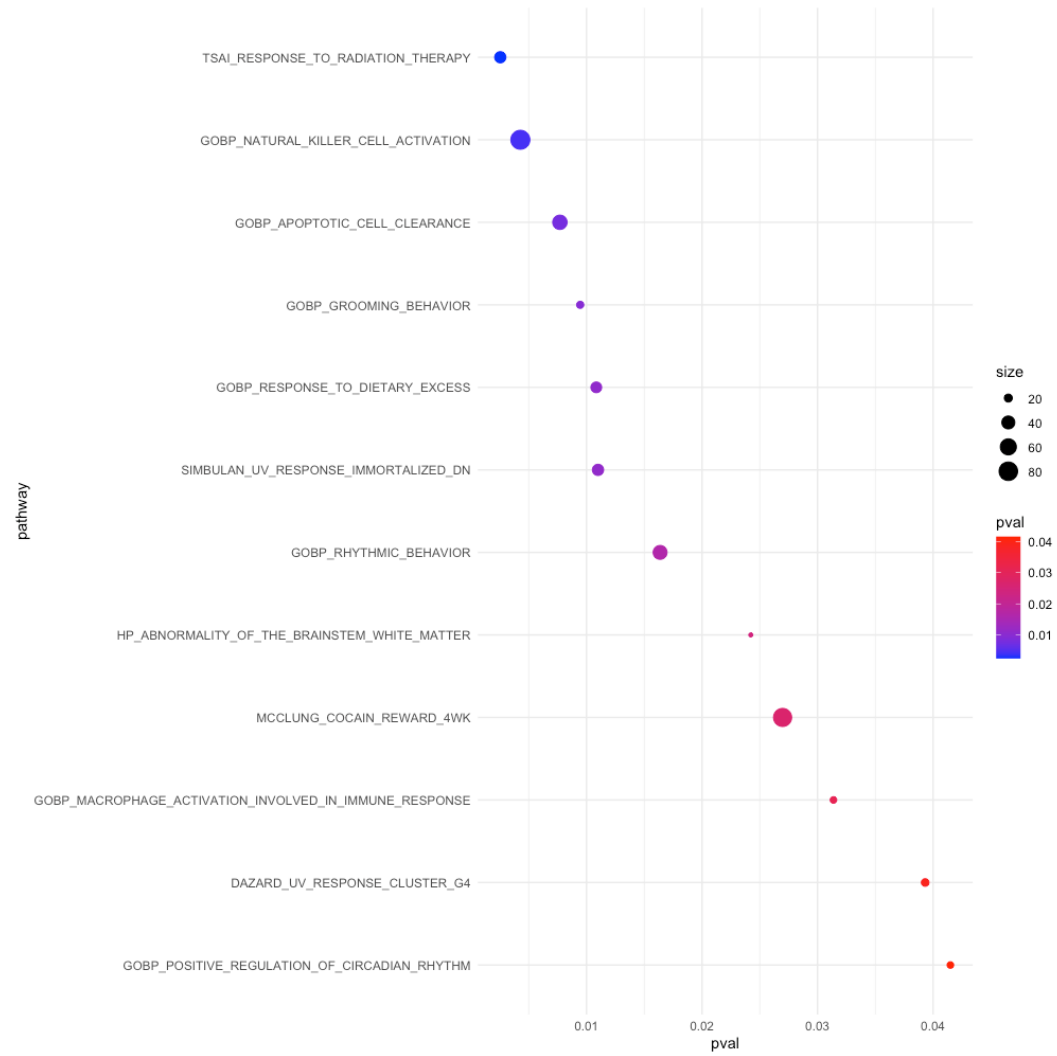


Figure S5. Dotplot presenting chosen significantly enriched pathways with p value < 0.05 , for one month after irradiation for hippocampus

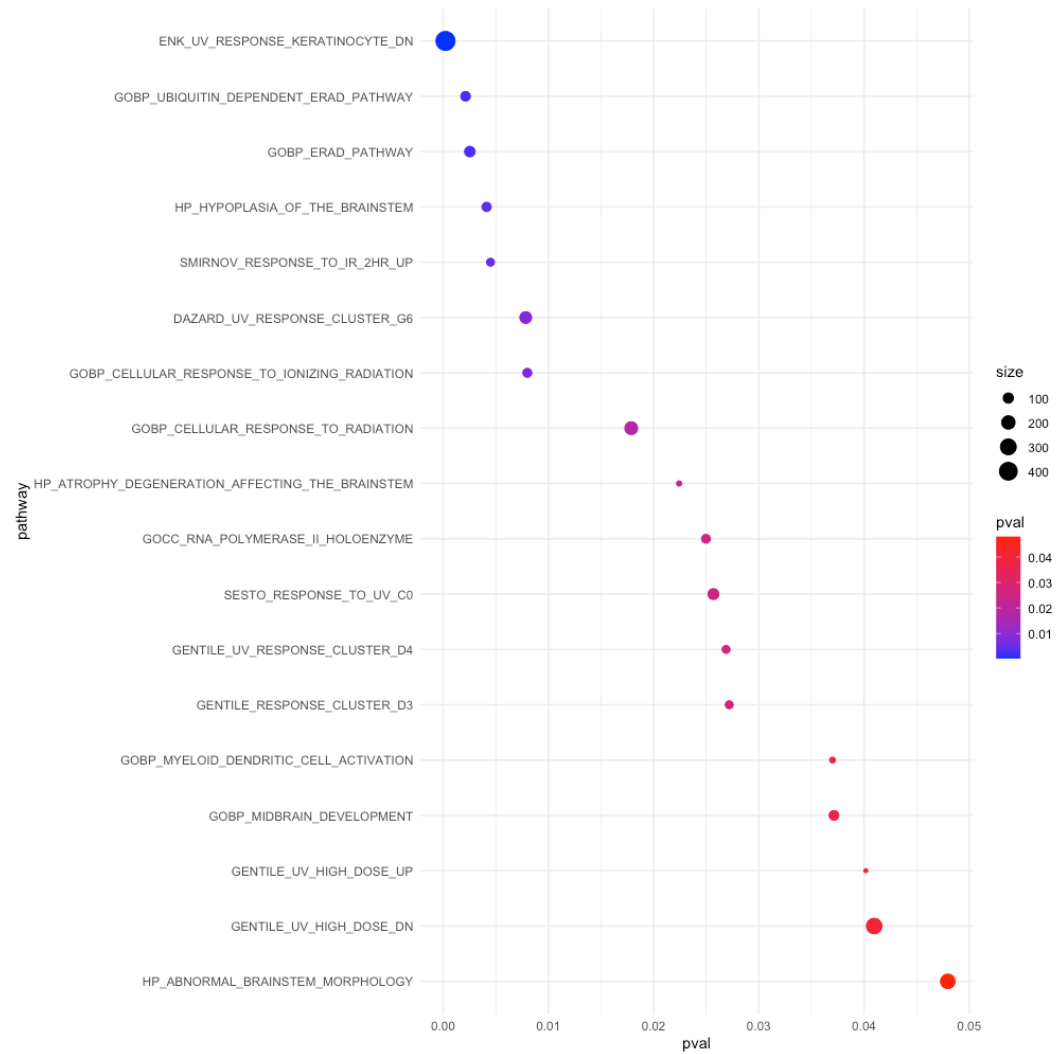


Figure S6. Dotplot presenting chosen significantly enriched pathways with p value < 0.05 , for six months after irradiation for hippocampus

Table S1 List of genes with a particular trend. for a specific brain region. after one month of exposure to radiation.

ascendingGenesCE1m	ascendingGenesCO1m	ascendingGenesHIP1m	descendingGenesCE1m	descendingGenesCO1m	descendingGenesHIP1m	UshapeCE1m	UshapeCO1m	UshapeHIP1m	NshapeCE1m	NshapeCO1m	NshapeHIP1m
170003D09Rik	1700055D18Rik	1700025F24Rik	1700123M08Rik	1700123M08Rik	1700123M08Rik	2810047C21Rik1	1700055D18Rik	1700016L21Rik	1700016L21Rik	1700016L21Rik	2310002F09Rik
A930033H14Rik	4930448C13Rik	A930012L18Rik	2310002F09Rik	2810047C21Rik1	Aard	1700080G11Rik	1700025F24Rik	1700028P15Rik	1700025F24Rik	1700052K11Rik	AY512915
Adams2	4930548K13Rik	A930033H14Rik	AY512915	A930012L18Rik	Aif1	4933428G20Rik	2310002F09Rik	1700055D18Rik	1700028P15Rik	Aif1	Apold1
Akap3	Accs	Accs	Aard	AY512915	Brme1	A930012L18Rik	3110004A20Rik	1700080G11Rik	1700052K11Rik	Alg13	Asc3
Alg13	Adams2	Akap3	Ccl11	Aard	Ccl22	Arfrp1	4930524J08Rik	1700123M08Rik	4930548K13Rik	Asb17	C630031E19Rik
Avp1	BC064078	Asb8	Crnde	Apold1	Crnde	BE692007	4933405L10Rik	3110004A20Rik	4933405L10Rik	Asb8	CommD10
BC052688	Ccl11	Aunip	Eif1ad	Arfrp1	Gm10731	Brme1	4933428G20Rik	4930524J08Rik	Asb17	Asc3	D1Pas1
Bend3	Ces2f	BC052688	Gm11266	Aunip	Glyr1	CN725425	A930033H14Rik	Abcg2	Asc3	Ceacam-ps1	Ecrg4
Ccl22	Eif1ad	Cfap36	Gm10731	Avp1	Gm11267	Cfap36	Ag04	Ag04	Ctdp1	Chrd1	Eef1akmt1
Cdk11b	Foxn2	Ctdp1	Gm10791	Cdk11b	Gm15587	CommD10	BE692007	Arfrp1	Cyp26a1	Ecrg4	Foxn2
Cyp2d26	Garin2	Cyp2d26	Gm11267	Dhdds	Gm15589	Ecrg4	Bend3	Asb17	Dhdds	Eef1akmt1	Gm22187
Fam163b	Gm10791	Dhdds	Gm11954	Esf1	Gm16223	Eftud2	Brme1	Avp1	Gm14936	Eftud2	Gm22345
Gm13398	Gm13398	Dusp15	Gm20110	F630040K05Rik	Gm16279	Foxn2	Cocd8	BE692007	Gm15587	Gm10126	Gm24043
Gm13974	Gm1604a	Eftud2	Gm22296	Fam163b	Gm16299	Fth1	CommD10	CN725425	Gm16299	Gm10731	Gm24285
Gm14167	Gm16279	Esf1	Gm23331	Fth1	Gm20110	Gm16223	Crnde	Ccl11	Gm17249	Gm15589	Gm25150
Gm16364	Gm20110	Fam163b	Gm24285	Gm13974	Gm22127	Gm16279	Dusp15	Cdk11b	Gm20026	Gm16982	Gm25152
Gm22004	Gm22004	Fyb1	Gm25622	Gm14936	Gm20751	Gm22544	Gm14167	Ces2f	Gm22127	Gm20026	Gm25811
Gm22544	Gm22127	Gm20026	Gm25919	Gm17249	Gm24949	Gm23460	Gm15587	Defb40	Gm22498	Gm24285	Gm26437
Gm23709	Gm22498	Gm22296	Gm26437	Gm22915	Gm25058	Gm24523	Gm16223	Egfl7	Gm23453	Gm25058	Gm50619
Gm24230	Gm23331	Gm23453	Gm57518	Gm23709	Gm25431	Gm24949	Gm20751	Eif1ad	Gm23895	Gm25269	Gm5451
Gm25152	Gm24230	Gm23453	Gm8700	Gm23895	Gm25600	Hmgb1	Gm22281	Fth1	Gm24043	Gm25431	Gm6605
Gm25431	Gm24523	Gm2710	Gm9234	Gm25150	Gm26367	Ighv1-74	Gm22296	Gm10791	Gm24481	Gm25622	Gm8700
Gm25811	Gm25811	Gm38388	Gsc	Gm26437	Herc6	Inka2	Gm24840	Gm11954	Gm25269	Gm38388	Ift46
Gm26367	Gm26367	Gsc	Lin54	Gm50619	Igfbp7	Lypd8	Gm25152	Gm14936	Gm25600	Gm47655	Igkv4-55
Gm38388	Gm5451	H2-Ab1	Or10n1	Gm5930	Ighv1-18	Mir25	Gm25802	Gm1604a	Gm26411	Gm9767	Mir25
Gm6605	Gm57518	Lin54	Or10p21	Hacd4	Ighv1-74	My4	Gm25924	Gm16364	Gm5766	Gsc	Mir5135
Lrrc32	Gm5766	Lypd8	Or52a5b	Herc6	Ighv9-3	Naa20	Gm6605	Gm17249	Gm7160	Igfbp7	Mrps14
Mark4	Gm7160	Mad211bp	Or8b55	Inka2	Or11i1	Gm7337	Mark4	Gm20751	Gm9767	Igkv4-55	Myh13
Mccc1	Gsta2	My4	Rpl39l	Mccc1	Meis1	Or2ak5	Hnf4g	Gm22915	H2-Ab1	Krtap19-1	Or10p21
Mir204	Hmgb1	Neo1	Stard8	Mill2	Mir1187	Or5p81	Hsd17b10	Gm23331	Hacd4	Mrps14	Or51a5
Mir5100	Ighv9-3	Nlrp4c	Sypc1-ps1	Myh13	Mir93	Or7g19	Ift46	Gm23460	Hnf4g	Nr5a2	Or52ab2
Mir763	Krtap11-1	Oga	Tdpoz3	Myom1	Myom1	Plkna4os1	Ighv1-18	Gm25802	Ighv9-3	Or10ak11	Or5p81
Muc20	Mir5100	Or4c1	Tex264	Myom1	Naa20	Pth2	Kif18b	Gm25919	Kif18b	Or13l2	Or6c3b
Myh13	Mir763	Or8k38	Traj61	Omp	Nodal	Rpia	Lypd8	Gm26411	Mad211bp	Or52a24	Or8b55
Ncapd3	Mir767	Phf6	Txlna	Or118	Npy6r	Sf3a3	Mark4	Gm5930	Mccc2	Or6c3b	Parm1
Nup210l	Muc20	Pradc1	Utp14b	Or51a5	Nr5a2	Spata25	Mccc2	Gsta2	Mill2	Pds5a	Pds5a
Oga	Nodal	Rhox4c	Or10n1	Or8k38	Vcf1	Tcof1	Mir1187	Hsd17b10	Mir1954	Phf6	Plscr111
Or13l2	Nup210l	Rpia	Wdr5b	Pantr1	Or118	Thoc2	Mir93	Mir1954	Mir767	Plscr111	Snord22
Or51a5	Oga	Spata25	Zfp1001	Peg13	Or2d2b	Thsd1	Ncapd3	Mir204	Mir93	Prr23a2	Tank
Or52a24	Or10p21	Stard8	Zfp422-ps	Rassf4	Or52a24	Tmem171	Neo1	Mrps36-ps1	Mrps14	Prss52	Tcf4
Or8k3	Or228	Sypc1-ps1	n-R5s5	Sec11c	Or5ac17	Trmt6	Nlrp4c	Ncapd3	Mrps36-ps1	Stard8	Tmem267
Oxct1as	Or52ab2	Tdpoz3		Snord22	Or7g19		Or10n1	Nup210l	Nlrp4c	Sypc1-ps1	Vmn1r43
Peg13	Or8b55	Tmem171		Tank	Pantr1		Or2ak5	Or10ak11	Npy6r	Tm4s14	Vmn2r109
Rufy4	Otub1	Tmprss9		Tcof1	Pantr1		Or2ak5	Or2d2b	Or2d2b	Txlna	Vmn2r77
Spata31g1	Parm1	Tti2		Vmn2r86	Pasma4		Or5ac17	Or52a5b	Or4c1	Utp14b	
Srsf5	Rpl39l	Txlna		Zfp276	Rpl39l		Or5p81	Otub1	Or52ab2	Vmn1r43	
Tas2r107	Spata25	Usp42			Tcl1b2		Pglyrp4	Peg13	Or6c3b	Vmn2r109	
Tcf4	Spinkl	Vmn1r32			Tcof1		Pasma4	Pglyrp4	Otub1	Zfp1001	
Tcl1b2	Tafazzin	Vmn2r15			Tm4s14		Spata31g1	Pltp	Pantr1	Zfp422-ps	
Tm4s14	Tmem171	Zfp1001					Srsf5	Prr23a2	Parm1		
Tti2	Tti8						Tcf4	Rprd2	Pds5a		
n-R5s65	Usp42						Tex264	Sf3a3	Pglyrp4		
	Vmn1r32						Thsd1	Snora20	Poteg		
	Vmn2r77						Tmprss9	Srsf5	Prrt1b		
							Traj61	Tas2r107	Ptchd4		
							Trmt6	Trim71	Rhox4c		
							Tti2	Trmt6	Snord22		
							Vcf1	Vcf1	Tank		
								Zfp276	Tmprss9		
								Zfp422-ps	Usp42		
								n-R5s65	Vmn1r32		
									Vmn1r43		
									Vmn2r109		

Table S2 List of genes with a particular trend. for a specific brain region. after six months of exposure to radiation.

ascendingGenesCE6m	ascendingGenesCO6m	ascendingGenesHIP6m	descendingGenesCE6m	descendingGenesCO6m	descendingGenesHIP6m	UshapeCE6m	UshapeCO6m	UshapeHIP6m	UshapeCE6m	UshapeCO6m	UshapeHIP6m
1700080G11Rik	A930033H14Rik	1700016L21Rik	1700016L21Rik	1700123M08Rik	4933405L10Rik	Arfrp1	1700016L21Rik	1700025F24Rik	1700055D18Rik	1700003D09Rik	1700080G11Rik
1700123M08Rik	Aard	2810047C21Rik1	4930448C13Rik	2310002F09Rik	4933428G20Rik	BE692007	1700025F24Rik	1700028P15Rik	2310002F09Rik	1700028P15Rik	2310002F09Rik
4930524J08Rik	Ago4	4930448C13Rik	Aard	3110004A20Rik	Aunip	Cyp26a1	1700055D18Rik	1700052K11Rik	3110004A20Rik	2810047C21Rik1	AY512915
4930548K13Rik	Arfrp1	4930548K13Rik	Asb17	4933405L10Rik	Dipk2a	Foxn2	4930524J08Rik	1700055D18Rik	AY512915	Aunip	Akap3
4933428G20Rik	Asb8	A930033H14Rik	Aunip	4933428G20Rik	E430024I08Rik	Gm16982	Apold1	1700123M08Rik	Accs	BE692007	CN725425
A930012L18Rik	Ceacam23	Accs	CN725425	A930012L18Rik	Esf1	Gm20026	BC064078	4930430F21Rik	Ceacam23	CFap36	Cdk11b
Adams2	D1Pas1	Ago4	Ccl11	AY512915	Fyb1	Gm20110	C630031E19Rik	4930524J08Rik	Comm10	Chrdl1	Ces2f
Ago4	Ecrq4	Alq13	Ccl22	Gm11954	Gm13398	Gm20751	CN725425	A930012L18Rik	Crnde	Dipk2a	Cfap36
Ctdp1	Eftud2	Avp1	CFap36	Accs	Gm13398	Gm22544	Crnde	Apold1	Gm11954	Eif1ad	Crnde
Cyp2d26	Egfl7	BE692007	Chrdl1	Asb17	Gm15587	Gm23453	Cyp26a1	Ceacam-ps1	Gm1604a	F630040K05Rik	Eftud2
Ecrq4	Fth1	Brme1	D1Pas1	BC052688	Gm16364	Gm24523	Gm1604a	Ceacam23	Gm17249	Fam163b	Egfl7
Eftud2	Gm10731	C630031E19Rik	Defb40	Bend3	Gm23460	Gm25622	Gm16279	Dusp15	Gm24230	Fyb1	Fth1
Egfl7	Gm14167	Ccdc8	Dipk2a	Ccdc8	Gm24043	Gm25811	Gm16364	Ecrq4	Gm25269	Glyr1	Garin2
Fam163b	Gm16223	Ctdp1	E430024I08Rik	Ctdp1	Gm26367	Gm25924	Gm16982	Eef1akmt1	Gm25919	Gm11266	Gm11266
Fyb1	Gm22127	Cyp26a1	Gm10466	Cyp2d26	Gm26437	Igf1bp7	Gm17249	F630040K05Rik	Gm5451	Gm13974	Gm14936
Gm13974	Gm22296	Dhdds	Gm10791	Gm20026	Gm38388	Kif18b	Gm20110	Foxn2	Gm57518	Gm25150	Gm20026
Gm14167	Gm22345	Eif1ad	Gm14936	Gm22004	H2-Ab1	Mark4	Gm20751	Gm14167	Gm6605	Gm3134	Gm22281
Gm16279	Gm22498	Fam163b	Gm22127	Gm24043	Hacd4	Mccc1	Gm22187	Gm15589	Gm7160	Gm8700	Gm22544
Gm22296	Gm24285	Gm11267	Gm22187	Gm24230	Inka2	Meis1	Gm22281	Gm16223	Gm9234	Gsta2	Gm25058
Gm22498	Gm25600	Gm13974	Gm23460	Gm24481	Kif18b	Milil2	Gm22481	Gm16279	Gsc	Herc6	Gm25431
Gm26411	Gm25802	Gm20110	Gm23709	Gm25622	Krtap19-1	Myom1	Gm23331	Gm16982	Herc6	Hsd17b10	Gm2710
Gm47655	Gm25811	Gm22127	Gm24043	Gm26411	Lin54	Npy6r	Gm23460	Gm17249	Hnf4g	Ighv1-18	Gm5930
Gm5766	Gm25919	Gm22296	Gm24285	Gm2710	Milil2	Nr5a2	Gm23709	Gm22345	Mir1187	Inka2	Gm6605
Ighv1-18	Gm26437	Gm22498	Gm24949	Gm47655	Mir1187	Or52a5b	Gm23895	Gm23709	Mir25	Myh13	Gm9767
Inka2	Ilt46	Gm22915	Gm50619	Gm25150	Mir93	Or7g19	Gm24523	Gm24230	Myl4	Myl4	Herc6
Lin54	Igf1bp7	Gm23331	Gm25431	Gm7160	Mrsps14	Pr72a2	Gm24840	Gm24285	Or2ak5	Oga	Hnf4g
Lrrc32	Kif18b	Gm25600	Gm25802	Gm2337	Muc20	Rpia	Gm25058	Gm25152	Or8b55	Or2ak5	Ighv9-3
Mir1954	Lypd8	Gm25802	Gm26367	Gm9767	Nodal	Snord22	Gm25269	Gm25269	Rassf4	Or7g19	Igkv4-55
Mir763	Mccc1	Gm25811	Gm2710	Gsc	Oga	Srsf5	Gm25431	Gm50619	Spata25	Or8k3	Lypd8
Mir93	Mccc2	Gm3134	Gm5930	Igkv4-55	Or4c1	Thsd1	Gm25924	Gm5451	Speer9-ps1	Peg13	Meis1
Naa20	Milil2	Gm47655	Gm7337	Gm47655	Lin54	Til2	Gm38388	Gm5451	Stard8	Rassf4	Or10ak11
Ncapd3	Mir1187	Gm7160	Krtap19-1	Lrrc32	Pds5a	Txlna	Gm5930	Ilt46	Tank	Rprd2	Or10n1
Nlrp4c	Naa20	Gm7337	Mir767	Mark4	Pglyrp4	Usp42	Hacd4	Igf1bp7	Tmprss9	Stard8	Pantr1
Omp	Nlrp4c	Gm8700	Mrsps14	Mir25	Poteg	Utp14b	Hnf4g	Ighv1-74	Tilil8	Traj61	Rhox4c
Or10n1	Or5p81	Gm9234	Mrsps36-ps1	Nodal	Prrt1b	Vmn2r77	Ighv1-74	Lrrc32	Zfp422-ps	Vcf1	Rpia
Or11i1	Or8b55	Hsd17b10	Myh13	Or11i1	Rufy4		Mir204	Mad211bp	n-R5s65	Vmn2r109	Sf3a3
Or52ab2	Otub1	Ighv1-18	Neo1	Or13i2	Sec11c		Mir763	Mir5135			Snord22
Oxct1as	Phf6	Mccc1	Nodal	Or2d2b	Spata31g1		Mir93	Mir763			Tm4sf4
Plxna4os1	Rpl39l	Mccc2	Or10p21	Or51a5	Tcof1		Muc20	Npy6r			Txlna
Prrt1b	Spink1	Mir1954	Or51a5	Or52a24	Tmem267		Ncapd3	Nr5a2			Vmn2r109
Snora20	Tafazzin	Mir204	Or52a24	Or52ab2	Tmprss9		Omp	Or10p21			
Spata31g1	Tank	Mir5100	Or6c3b	Or5ac17	Zfp422-ps		Or10ak11	Or13i2			
Spink1	Tas2r107	Mrsps36-ps1	Or8k38	Prrt1b	n-R5s5		Or10n1	Or2z8			
Tafazzin	Tdpoz3	Myh13	Pglyrp4	Rufy4	n-R5s65		Or10p21	Parm1			
Tcf4	Thoc2	My4	Plscr11i	Sf3a3			Or1l8	Plscr11i			
Tm4sf4	Thsd1	Myom1	Poteg	Speer9-ps1			Or2z8	Pltp			
Trim71	Tm4sf4	Nlrp4c	Ptchd4	Tcof1			Or52a5b	Pradc1			
Trmt6	Trmt6	Nup210l	Pthr2	Tmem267			Or8k38	Prr23a2			
Vmn2r109	Wdr5b	Or11i1	Rufy4	Utp14b			Oxct1as	Prss52			
Vmn2r86	Zfp1001	Or2ak5	Sf3a3	Vmn1r43			Pglyrp4	Pthr2			
Wdr5b	Zfp422-ps	Or2d2b	Sycp1-ps1	Vmn2r77			Pltp	Rassf4			
Zfp276		Or51a5	Tcof1	Vmn2r86			Pradc1	Rpl39l			
		Or52a24	Tdpoz3	n-R5s5			Ptchd4	Tank			
		Or52a5b	Tmem171				Rpia	Tex264			
		Or5ac17	Tmem267				Snora20	Vmn2r15			
		Or7g19	Zfp1001				Snord22	Zfp276			
		Or8k3	n-R5s5				Srsf5				
		Otub1					Tcl1b2				
		Oxct1as					Tex264				
		Plxna4os1					Tilil8				
		Psm4					Txlna				
		Ptchd4					n-R5s65				
		Rprd2									
		Speer9-ps1									
		Tas2r107									

ascendingGenesCE6m	ascendingGenesCO6m	ascendingGenesHIP6m	descendingGenesCE6m	descendingGenesCO6m	descendingGenesHIP6m	UshapeCE6m	UshapeCO6m	UshapeHIP6m	∩shapeCE6m	∩shapeCO6m	∩shapeHIP6m
		Tdpoz3									
		Traj61									
		Tti2									
		Usp42									
		Vcf1									
		Vmn2r86									
		Wdr5b									

Table S3 Selected radiation-specific significant gene sets after GSEA, for cerebellum after one month of radiation exposure.

<i>pathway</i>	<i>pval</i>	<i>fdr</i>	<i>log2err</i>	<i>ES</i>	<i>NES</i>	<i>size</i>
MONNIER_POSTRADIATION_TUMOR_ESCAPE_DN	0.033966034	0.322177822	0.245041785	0.354919345	1.114185484	380
HP_ABNORMAL_AGGRESSIVE_IMPULSIVE_OR_VIOLENT_BEHAVIOR	0.023881168	0.322177822	0.352487858	0.360232821	1.128615482	348
HP_SPECIFIC_LEARNING_DISABILITY	0.025683497	0.322177822	0.352487858	0.373716324	1.158964514	246
DACOSTA_UV_RESPONSE_VIA_ERCC3_UP	0.009191707	0.270341171	0.380730401	0.375425976	1.172239781	306
HP_ABNORMAL_CNS_MYELINATION	0.004201468	0.225828894	0.407017919	0.380881784	1.186471926	293
HP_AGGRESSIVE_BEHAVIOR	0.00844443	0.270341171	0.380730401	0.383464789	1.185567285	231
HP_ABNORMAL_SOCIAL_BEHAVIOR	0.022980004	0.322177822	0.352487858	0.383916041	1.180532579	199
LEIN_MIDBRAIN_MARKERS	0.010835718	0.291209924	0.380730401	0.43222873	1.277970006	83
KIM_ALL_DISORDERS_DURATION_CORR_DN	0.000645701	0.149405595	0.477270815	0.44172103	1.335387542	139
HP_INAPPROPRIATE_BEHAVIOR	0.032967033	0.322177822	0.248911114	0.452530886	1.293058818	51
GOBP_SENSORY_PERCEPTION_OF_TASTE	0.027786217	0.322177822	0.352487858	0.457910717	1.310106644	52
GOBP_MICROGLIAL_CELL_ACTIVATION	0.031968032	0.322177822	0.252961123	0.458315847	1.298119984	43
LEIN_PONS_MARKERS	0.002016416	0.162573561	0.431707696	0.458467311	1.358726172	91
WP_NEURODEGENERATION_WITH_BRAIN_IRON_ACCUMULATION_NBIA_SUBTYPES_PATHWAY	0.031968032	0.322177822	0.252961123	0.45857068	1.299332761	44
MCCLUNG_DELTA_FOSB_TARGETS_2WK	0.013824839	0.307483498	0.380730401	0.472234124	1.348459241	50
LEIN_OLIGODENDROCYTE_MARKERS	0.00129778	0.149405595	0.455059867	0.477965072	1.405487697	77
GOBP_LONG_TERM_MEMORY	0.027972028	0.322177822	0.271288555	0.480561132	1.338666138	35
REACTOME_DNA_DAMAGE_RECOGNITION_IN_GG_NER	0.026284274	0.322177822	0.352487858	0.480715015	1.350414748	38
GOBP_SENSORY_PERCEPTION_OF_BITTER_TASTE	0.017272647	0.322177822	0.352487858	0.4979942	1.38439026	34
HP_PROGRESSIVE_NEUROLOGIC_DETERIORATION	0.002645375	0.18958518	0.431707696	0.504122292	1.439515547	50
LEIN_LOCALIZED_TO_PROXIMAL_DENDRITES	0.009640073	0.270341171	0.380730401	0.512685863	1.432533397	36
JOHANSSON_GLIOMAGENESIS_BY_PDGFB_DN	0.042296073	0.363746224	0.219250347	0.52270833	1.365622824	20
HP_ADDICTIVE_BEHAVIOR	0.029948776	0.322177822	0.352487858	0.539378548	1.435418228	23
HP_ABNORMAL_METABOLIC_BRAIN_IMAGING_BY_MRS	0.004796351	0.237972816	0.407017919	0.544114409	1.505110857	32
GOBP_BEHAVIORAL_RESPONSE_TO_PAIN	0.035425101	0.322177822	0.241339977	0.559469183	1.41982836	16

<i>pathway</i>	<i>pval</i>	<i>fdr</i>	<i>log2err</i>	<i>ES</i>	<i>NES</i>	<i>size</i>
<i>GOBP_AXON_ENSHEATHMENT_IN_CENTRAL_NERVOUS_SYSTEM</i>	0.007488302	0.270341171	0.407017919	0.58328874	1.552273987	23
<i>HP_ABNORMAL_BRAIN_LACTATE_LEVEL_BY_MRS</i>	0.015994415	0.322177822	0.352487858	0.601578599	1.51573933	15
<i>GOBP_EMBRYONIC_BRAIN_DEVELOPMENT</i>	0.007774827	0.270341171	0.407017919	0.607871761	1.567979871	18

Table S4 Selected radiation-specific significant gene sets after GSEA, for cerebellum after six months of radiation exposure.

pathway	pval	fdr	log2err	ES	NES	size
<i>BRUINS_UVC_RESPONSE_EARLY_LATE</i>	0.000271139	0.006319346	0.498493109	0.370990341	1.269016017	311
<i>BYSTRYKH_HEMATOPOIESIS_STEM_CELL_AND_BRAIN_QTL_TRANS</i>	0.010387351	0.056778316	0.380730401	0.373165752	1.237698937	159
<i>CHESLER_BRAIN_HIGHEST_EXPRESSION</i>	0.047952048	0.136854296	0.204294757	0.435301163	1.30342004	37
<i>DACOSTA_UV_RESPONSE_VIA_ERCC3_COMMON_DN</i>	1.41164E-13	9.10511E-11	0.943632225	0.430902957	1.491534499	461
<i>DACOSTA_UV_RESPONSE_VIA_ERCC3_TTD_DN</i>	0.004870712	0.03611045	0.407017919	0.428469493	1.369647111	84
<i>DACOSTA_UV_RESPONSE_VIA_ERCC3_UP</i>	0.01787342	0.07896134	0.352487858	0.341204711	1.166358442	306
<i>DACOSTA_UV_RESPONSE_VIA_ERCC3_XPCS_DN</i>	2.47137E-05	0.00122618	0.575610261	0.49286874	1.575505976	84
<i>DAZARD_RESPONSE_TO_UV_NHEK_DN</i>	5.88009E-09	1.26422E-06	0.761460801	0.427044817	1.456769478	296
<i>DAZARD_RESPONSE_TO_UV_SCC_DN</i>	0.006283566	0.042662105	0.407017919	0.399200891	1.302393483	115
<i>DAZARD_UV_RESPONSE_CLUSTER_G6</i>	4.29365E-05	0.001730876	0.557332239	0.429934851	1.419757352	144
<i>ENK_UV_RESPONSE_EPIDERMIS_DN</i>	0.0001213	0.003556292	0.538434096	0.358704503	1.244715526	499
<i>ENK_UV_RESPONSE_EPIDERMIS_UP</i>	0.031968032	0.107392607	0.252961123	0.337161046	1.147919686	288
<i>ENK_UV_RESPONSE KERATINOCYTE_DN</i>	5.91745E-07	9.29013E-05	0.659444398	0.381451985	1.321285678	468
<i>GENTILE_UV_HIGH_DOSE_DN</i>	0.000407845	0.007470507	0.498493109	0.371061094	1.262747279	284
<i>GENTILE_UV_RESPONSE_CLUSTER_D4</i>	0.00464763	0.035687161	0.407017919	0.46423569	1.43638727	53
<i>GENTILE_UV_RESPONSE_CLUSTER_D6</i>	0.045	0.135630841	0.211400189	0.447385237	1.324965816	34
<i>GENTILE_UV_RESPONSE_CLUSTER_D8</i>	0.006209205	0.042662105	0.407017919	0.49594922	1.485018206	37
<i>GOBP_CELLULAR_RESPONSE_TO_GAMMA_RADIATION</i>	0.046	0.136728111	0.208955028	0.464445188	1.335493664	27
<i>GOBP_CELLULAR_RESPONSE_TO_IONIZING_RADIATION</i>	0.002127409	0.022494731	0.431707696	0.442534564	1.39834925	72
<i>GOBP_CEREBELLAR_CORTEX_FORMATION</i>	0.028028028	0.10099485	0.271288555	0.48839822	1.387460335	25
<i>GOBP_COGNITION</i>	0.002016416	0.022043873	0.431707696	0.359837824	1.229761333	301
<i>GOBP_CYTOPLASMIC_PATTERN_RECOGNITION_RECEPTOR_SIGNALING_PATHWAY</i>	0.001500267	0.018973967	0.455059867	0.467342864	1.462319447	61
<i>GOBP_CYTOPLASMIC_PATTERN_RECOGNITION_RECEPTOR_SIGNALING_PATHWAY_IN_RESPONSE_TO_VIRUS</i>	0.009350503	0.054172108	0.380730401	0.502796039	1.489069171	34
<i>GOBP_ERAD_PATHWAY</i>	0.017272647	0.076833498	0.352487858	0.384374022	1.247885044	107
<i>GOBP_HINDBRAIN_DEVELOPMENT</i>	0.037130842	0.116826308	0.321775918	0.362766785	1.198487424	147

pathway	pval	fdr	log2err	ES	NES	size
<i>GOBP_LEARNING</i>	0.047952048	0.136854296	0.204294757	0.355076007	1.172226993	143
<i>GOBP_MACROPHAGE_ACTIVATION_INVOLVED_IN_IMMUNE_RESPONSE</i>	0.038461538	0.120425691	0.23112671	0.5200985	1.399406851	17
<i>GOBP_MEMORY</i>	0.032300928	0.107392607	0.321775918	0.374483961	1.225646838	122
<i>GOBP_POSITIVE_REGULATION_OF_MACROAUTOPHAGY</i>	0.001702755	0.019892918	0.455059867	0.461026278	1.455724422	71
<i>GOBP_REGULATION_OF_DNA_TEMPLATED_TRANSCRIPTION_IN_RESPONSE_TO_STRESS</i>	0.013227015	0.064146048	0.380730401	0.442729132	1.369844034	53
<i>GOBP_REGULATION_OF_NEUROGENESIS</i>	0.005391236	0.039515312	0.407017919	0.34777062	1.194321317	350
<i>GOBP_REGULATION_OF_PATTERN_RECOGNITION_RECEPTOR_SIGNALING_PATHWAY</i>	0.040959041	0.125802769	0.222056046	0.376624256	1.218414989	101
<i>GOBP_REGULATION_OF_RIG_I_SIGNALING_PATHWAY</i>	0.01653669	0.075198315	0.352487858	0.53813601	1.483586683	20
<i>GOBP_REGULATION_OF_VIRAL_INDUCED_CYTOPLASMIC_PATTERN_RECOGNITION_RECEPTOR_SIGNALING_PATHWAY</i>	0.003176034	0.028062216	0.431707696	0.559999727	1.573069647	23
<i>GOBP_RESPONSE_TO_GAMMA_RADIATION</i>	0.010985174	0.059172644	0.380730401	0.446123647	1.38034697	53
<i>GOBP_RESPONSE_TO_IONIZING_RADIATION</i>	0.001334596	0.017216285	0.455059867	0.406627687	1.340760362	139
<i>GOBP_RESPONSE_TO_RADIATION</i>	0.007175897	0.044936441	0.407017919	0.339154782	1.171903241	424
<i>GOBP_RHYTHMIC_BEHAVIOR</i>	0.022980004	0.092638141	0.352487858	0.445302437	1.361399722	45
<i>GOBP_RIG_I_SIGNALING_PATHWAY</i>	0.01310374	0.064029637	0.380730401	0.499898858	1.444136067	28
<i>GOBP_SENSORY_PERCEPTION_OF_MECHANICAL_STIMULUS</i>	0.026973027	0.098291539	0.276500599	0.3582989	1.194262634	174
<i>GOBP_UBIQUITIN_DEPENDENT_ERAD_PATHWAY</i>	0.006581009	0.04376032	0.407017919	0.420699937	1.34481092	84
<i>GOCC_MYELIN_SHEATH</i>	0.040959041	0.125802769	0.222056046	0.421784901	1.284998867	44
<i>GOCC_RNA_POLYMERASE_II_HOLOENZYME</i>	0.028971029	0.102213115	0.266350657	0.40193399	1.266415431	69
<i>GSE29949_DC_BRAIN_VS_MONOCYTE_BONE_MARROW_UP</i>	0.000746448	0.011742894	0.477270815	0.385600842	1.290876419	196
<i>GSE29949_MICROGLIA_VS_DC_BRAIN_UP</i>	0.004796351	0.035972635	0.407017919	0.373244351	1.250112366	199
<i>HP_ABNORMALITY_OF_THE_BRAINSTEM_WHITE_MATTER</i>	0.025562372	0.097402597	0.287857117	0.549571795	1.446514732	15
<i>HP_ABNORMAL_AGGRESSIVE_IMPULSIVE_OR_VIOLENT_BEHAVIOR</i>	1.03532E-06	9.53975E-05	0.643551836	0.397432159	1.364385396	348
<i>HP_ABNORMAL_BRAINSTEM_MORPHOLOGY</i>	0.003089347	0.027675399	0.431707696	0.363459974	1.229072638	242
<i>HP_ABNORMAL_CONSUMPTION_BEHAVIOR</i>	0.001757979	0.019892918	0.455059867	0.40755845	1.341440846	134
<i>HP_ABNORMAL_EATING_BEHAVIOR</i>	0.000307594	0.006399932	0.498493109	0.442369267	1.429871128	100
<i>HP_ABNORMAL_FEAR_ANXIETY_RELATED_BEHAVIOR</i>	7.16323E-05	0.002310143	0.538434096	0.373713587	1.289569101	392
<i>HP_ABNORMAL_SOCIAL_BEHAVIOR</i>	0.016071103	0.074041866	0.352487858	0.360634326	1.207877436	199

pathway	pval	fd	log2err	ES	NES	size
<i>HP_AGGRESSIVE_BEHAVIOR</i>	0.001113701	0.014965357	0.455059867	0.378347283	1.277176893	231
<i>HP_BENIGN_NEOPLASM_OF_THE_CENTRAL_NERVOUS_SYSTEM</i>	0.01262919	0.063639277	0.380730401	0.405498521	1.302079465	89
<i>HP_GLOBAL_BRAIN_ATROPHY</i>	0.046953047	0.136854296	0.206587923	0.406428934	1.262999011	55
<i>HP_INAPPROPRIATE_BEHAVIOR</i>	0.043956044	0.13373419	0.213927855	0.413096524	1.273331243	51
<i>HP_OBSESSIVE_COMPULSIVE_BEHAVIOR</i>	0.000284809	0.006319346	0.498493109	0.432321898	1.416857428	126
<i>HP_SELF_INJURIOUS_BEHAVIOR</i>	6.60175E-06	0.000473125	0.610526878	0.428069437	1.429807128	179
<i>HP_SPECIFIC_LEARNING_DISABILITY</i>	0.015169946	0.071945702	0.380730401	0.349567588	1.182496215	246
<i>JOHANSSON_BRAIN_CANCER_EARLY_VS_LATE_DN</i>	0.048951049	0.138479941	0.202071709	0.422060458	1.282799695	43
<i>KYNG_DNA_DAMAGE_BY_GAMMA_RADIATION</i>	0.04995005	0.139426901	0.199915231	0.387172494	1.226990279	75
<i>LEIN_CEREBELLUM_MARKERS</i>	0.006283566	0.042662105	0.407017919	0.414880753	1.327343477	85
<i>LEIN_LOCALIZED_TO_PROXIMAL_DENDRITES</i>	0.004721991	0.035831577	0.407017919	0.498999697	1.489541923	36
<i>LEIN_NEURON_MARKERS</i>	0.000412402	0.007470507	0.498493109	0.474313343	1.489483892	66
<i>LEIN_PONS_MARKERS</i>	0.024975025	0.096460426	0.287857117	0.389706086	1.252551103	91
<i>MCCLUNG_DELTA_FOSB_TARGETS_8WK</i>	0.019675741	0.08294675	0.352487858	0.436510452	1.341048426	49
<i>MEISSNER_BRAIN_ICP_WITH_H3K4ME3</i>	0.002057525	0.02211839	0.431707696	0.539488366	1.564250279	29
<i>MONNIER_POSTRADIATION_TUMOR_ESCAPE_DN</i>	0.000100962	0.003100964	0.538434096	0.366469182	1.263092208	380
<i>MONNIER_POSTRADIATION_TUMOR_ESCAPE_UP</i>	1.82203E-11	5.87605E-09	0.863415392	0.428485608	1.479552326	397
<i>RASHI_RESPONSE_TO_IONIZING_RADIATION_4</i>	0.006952814	0.04484565	0.407017919	0.457605198	1.405855755	49
<i>REACTOME_ACTIVATION_OF_ANTERIOR_HOX_GENES_IN_HINDBRAIN_DEVELOPMENT_DURING_EARLY_EMBRYOGENESIS</i>	0.01113463	0.059172644	0.380730401	0.401208544	1.295330572	97
<i>SESTO_RESPONSE_TO_UV_C2</i>	0.008743341	0.051738117	0.380730401	0.445928717	1.385746637	55
<i>SESTO_RESPONSE_TO_UV_C3</i>	0.045408678	0.136226034	0.211400189	0.493126595	1.359500266	20
<i>SESTO_RESPONSE_TO_UV_C5</i>	0.031968032	0.107392607	0.252961123	0.423665274	1.297827473	46
<i>SESTO_RESPONSE_TO_UV_C8</i>	0.009938984	0.054791834	0.380730401	0.433378855	1.368425649	71
<i>SIMBULAN_UV_RESPONSE_IMMORTALIZED_DN</i>	0.029	0.102213115	0.266350657	0.467432066	1.367999187	31
<i>WP_NEURODEGENERATION_WITH_BRAIN_IRON_ACCUMULATION_NBIA_SUBTYPES_PATHWAY</i>	0.019074967	0.081479162	0.352487858	0.447064966	1.362016456	44

Table S5 Selected radiation-specific significant gene sets after GSEA, for cortex after one month of exposure to radiation.

<i>pathway</i>	<i>pval</i>	<i>fdr</i>	<i>log2err</i>	<i>ES</i>	<i>NES</i>	<i>size</i>
DACOSTA_UV_RESPONSE_VIA_ERCC3_COMMON_DN	0.044955045	0.630347913	0.211400189	0.356827413	1.100482731	461
DAZARD_RESPONSE_TO_UV_SCC_DN	0.002978354	0.326548854	0.431707696	0.440936133	1.300033183	115
DAZARD_UV_RESPONSE_CLUSTER_G28	0.010471035	0.557091029	0.380730401	0.619162354	1.533723059	16
GENTILE_UV_RESPONSE_CLUSTER_D4	0.025974026	0.557091029	0.28201335	0.467146368	1.312828718	53
GENTILE_UV_RESPONSE_CLUSTER_D9	0.026052104	0.557091029	0.28201335	0.524790232	1.363569623	25
GHANDHI_BYSTANDER_IRRADIATION_UP	0.000339492	0.093143577	0.498493109	0.500068527	1.436608011	76
GHANDHI_DIRECT_IRRADIATION_UP	0.017573033	0.557091029	0.352487858	0.435215811	1.266617492	93
GOBP_FOREBRAIN_NEURON_DEVELOPMENT	0.025100402	0.557091029	0.287857117	0.54081297	1.388069684	22
GOBP_GAMMA_DELTA_T_CELL_ACTIVATION	0.013019145	0.557091029	0.380730401	0.579079088	1.459811167	19
GOBP_LEARNING	0.037962038	0.569430569	0.23112671	0.396338914	1.18115404	143
GOBP_LONG_TERM_MEMORY	0.02997003	0.557091029	0.261663522	0.491784637	1.331184616	35
GOBP_RESPONSE_TO_GAMMA_RADIATION	0.030969031	0.557091029	0.257206466	0.457779467	1.286504772	53
GOBP_VOCALIZATION_BEHAVIOR	0.000231981	0.093143577	0.518848078	0.71582526	1.773166118	16
GOCC_AMPA_GLUTAMATE_RECEPTOR_COMPLEX	0.003543941	0.326548854	0.431707696	0.584896393	1.524646224	26
GOCC_TRANSCRIPTION_FACTOR_TFIID_COMPLEX	0.040959041	0.600422305	0.222056046	0.495278316	1.319607487	31
KYNG_ENVIRONMENTAL_STRESS_RESPONSE_NOT_BY_GAMMA_IN_OLD	0.011606187	0.557091029	0.380730401	0.542103577	1.425744869	28
MCCLUNG_COCAIN_REWARD_4WK	0.012330278	0.557091029	0.380730401	0.447288542	1.284980494	76
MONNIER_POSTRADIATION_TUMOR_ESCAPE_DN	0.006283566	0.506612492	0.407017919	0.380380459	1.170276835	380
MURAKAMI_UV_RESPONSE_24HR	0.043259557	0.620053655	0.216542837	0.537918987	1.356049906	19
RASHI_RESPONSE_TO_IONIZING_RADIATION_1	0.026973027	0.557091029	0.276500599	0.484179334	1.321040358	39

Table S6 Selected radiation-specific significant gene sets after GSEA, for cortex after six months of exposure to radiation.

<i>pathway</i>	<i>pval</i>	<i>fdr</i>	<i>log2err</i>	<i>ES</i>	<i>NES</i>	<i>size</i>
<i>BRUINS_UVC_RESPONSE_EARLY_LATE</i>	0.006804092	0.091288235	0.407017919	0.353000782	1.193173679	311
<i>BRUINS_UVC_RESPONSE_VIA_TP53_GROUP_C</i>	0.026284274	0.180339771	0.352487858	0.395983818	1.256561353	89
<i>DACOSTA_UV_RESPONSE_VIA_ERCC3_COMMON_DN</i>	3.53725E-07	0.000227799	0.67496286	0.390540954	1.33827574	461
<i>DAZARD_RESPONSE_TO_UV_NHEK_DN</i>	9.15535E-07	0.000294802	0.659444398	0.410227435	1.385143513	296
<i>DAZARD_RESPONSE_TO_UV_SCC_DN</i>	0.000966438	0.033447929	0.477270815	0.42819065	1.38518469	115
<i>DAZARD_UV_RESPONSE_CLUSTER_G6</i>	0.008145521	0.097142875	0.380730401	0.384522296	1.259441504	144
<i>ENK_UV_RESPONSE_EPIDERMIS_DN</i>	0.002386391	0.054887001	0.431707696	0.342905205	1.17811725	499
<i>ENK_UV_RESPONSE_KERATINOCYTE_DN</i>	0.005391236	0.081938706	0.407017919	0.340444482	1.167186654	468
<i>GENTILE_UV_HIGH_DOSE_DN</i>	0.007547702	0.097142875	0.407017919	0.356347149	1.201601776	284
<i>GENTILE_UV_RESPONSE_CLUSTER_D8</i>	0.004503408	0.074363972	0.407017919	0.506500349	1.486070834	37
<i>GOBP_CELL_PROLIFERATION_IN_FOREBRAIN</i>	0.004890253	0.078733079	0.407017919	0.567621825	1.570352712	23
<i>GOBP_CENTRAL_NERVOUS_SYSTEM_NEURON_AXONOGENESIS</i>	0.017891293	0.15059975	0.352487858	0.480064072	1.400488647	35
<i>GOBP_CENTRAL_NERVOUS_SYSTEM_NEURON_DIFFERENTIATION</i>	0.014721577	0.142939488	0.380730401	0.371196329	1.225705731	169
<i>GOBP_CENTRAL_NERVOUS_SYSTEM_PROJECTION_NEURON_AXONOGENESIS</i>	0.03109328	0.189476482	0.257206466	0.501224378	1.410295159	26
<i>GOBP_IMMUNOLOGICAL_MEMORY_PROCESS</i>	0.038500507	0.206619385	0.23112671	0.535797672	1.41355741	17
<i>GOBP_MIDBRAIN_DOPAMINERGIC_NEURON_DIFFERENTIATION</i>	0.035460993	0.200323504	0.241339977	0.542928398	1.432369904	17
<i>GOBP_NATURAL_KILLER_CELL_MEDIATED_IMMUNITY</i>	0.032967033	0.196777778	0.248911114	0.407597607	1.270516791	69
<i>GOBP_NEURAL_TUBE_FORMATION</i>	0.035964036	0.201398601	0.237793834	0.383588433	1.231150133	103
<i>GOBP_OLFACTORY_LOBE_DEVELOPMENT</i>	0.04	0.209430894	0.224966094	0.462988992	1.350675597	35
<i>GOBP_POSITIVE_REGULATION_OF_MACROAUTOPHAGY</i>	0.014422665	0.142895323	0.380730401	0.42612352	1.331785902	71
<i>GOBP_RESPONSE_TO_LIGHT_STIMULUS</i>	0.007697156	0.097142875	0.407017919	0.350962919	1.185303232	298
<i>HP_ABNORMAL_AGGRESSIVE_IMPULSIVE_OR_VIOLENT_BEHAVIOR</i>	0.001095293	0.035268438	0.455059867	0.362416739	1.230726326	348
<i>HP_ABNORMAL_BRAINSTEM_MORPHOLOGY</i>	0.016371489	0.148496319	0.352487858	0.355349124	1.190302725	242
<i>HP_ABNORMAL_BRAINSTEM_MRI_SIGNAL_INTENSITY</i>	0.008004062	0.097142875	0.380730401	0.500338031	1.460516032	36
<i>HP_ABNORMAL_BRAIN_POSITRON_EMISSION_TOMOGRAPHY</i>	0.030090271	0.188137227	0.261663522	0.507406577	1.40376437	23

<i>pathway</i>	<i>pval</i>	<i>fdr</i>	<i>log2err</i>	<i>ES</i>	<i>NES</i>	<i>size</i>
<i>HP_ABNORMAL_CNS_MYELINATION</i>	0.00029848	0.014786237	0.498493109	0.378836852	1.279058939	293
<i>HP_ABNORMAL_FEAR_ANXIETY_RELATED_BEHAVIOR</i>	0.010237895	0.109886741	0.380730401	0.342120254	1.165860549	392
<i>HP_ABNORMAL_SOCIAL_BEHAVIOR</i>	3.90077E-05	0.00448803	0.557332239	0.414136515	1.375934785	199
<i>HP_DELAYED_CNS_MYELINATION</i>	0.030969031	0.189476482	0.257206466	0.396260282	1.251795291	80
<i>HP_FOCAL_T2_HYPERINTENSE_BRAINSTEM_LESION</i>	0.002502384	0.05557018	0.431707696	0.544420023	1.548526841	29
<i>HP_SELF_INJURIOUS_BEHAVIOR</i>	0.001353004	0.041492111	0.455059867	0.393480647	1.303086053	179
<i>JOHANSSON_GLIOMAGENESIS_BY_PDGFBDN</i>	0.031187123	0.189476482	0.257206466	0.51727529	1.400449757	20
<i>LEIN_LOCALIZED_TO_DISTAL_AND_PROXIMAL_DENDRITES</i>	0.004261063	0.072464035	0.407017919	0.603600011	1.592435564	17
<i>LEIN_NEURON_MARKERS</i>	0.000139438	0.009977542	0.518848078	0.49652346	1.54316729	66
<i>LIU_IL13_MEMORY_MODEL_UP</i>	0.026342452	0.180339771	0.28201335	0.554069655	1.461763101	17
<i>MONNIER_POSTRADIATION_TUMOR_ESCAPE_DN</i>	0.000293923	0.014786237	0.498493109	0.368489433	1.254467253	380
<i>MONNIER_POSTRADIATION_TUMOR_ESCAPE_UP</i>	5.3039E-05	0.00487959	0.557332239	0.373821079	1.274385617	397
<i>MURAKAMI_UV_RESPONSE_24HR</i>	0.005429203	0.081938706	0.407017919	0.575433974	1.546504657	19
<i>MURAKAMI_UV_RESPONSE_6HR_DN</i>	0.027162978	0.180339771	0.276500599	0.529295849	1.432993722	20
<i>RASHI_RESPONSE_TO_IONIZING_RADIATION_4</i>	0.03996004	0.209430894	0.224966094	0.429306729	1.295927909	49
<i>REACTOME_CARGO_RECOGNITION_FOR_CLATHRIN_MEDIATED_ENDOCYTOSIS</i>	0.008743341	0.098740699	0.380730401	0.405484948	1.301428312	103
<i>REACTOME_DNA_DAMAGE_RECOGNITION_IN_GG_NER</i>	0.033	0.196777778	0.248911114	0.464556569	1.366295575	38
<i>SESTO_RESPONSE_TO_UV_C1</i>	0.003570318	0.067626016	0.431707696	0.449078398	1.401601395	70
<i>SESTO_RESPONSE_TO_UV_C2</i>	0.006432288	0.088136025	0.407017919	0.461092224	1.406398961	55

Table S7 Selected radiation-specific significant gene sets after GSEA, for hippocampus after one month of exposure to radiation.

<i>pathway</i>	<i>pval</i>	<i>fdr</i>	<i>log2err</i>	<i>ES</i>	<i>NES</i>	<i>size</i>
DAZARD_UV_RESPONSE_CLUSTER_G4	0.039314516	1	0.227987203	0.54322928	1.369222262	19
GOBP_APOPTOTIC_CELL_CLEARANCE	0.007697156	0.883816287	0.407017919	0.494275389	1.369401643	48
GOBP_GROOMING_BEHAVIOR	0.009454503	0.883816287	0.380730401	0.593890009	1.484238062	18
GOBP_MACROPHAGE_ACTIVATION_INVOLVED_IN_IMMUNE_RESPONSE	0.031376518	1	0.257206466	0.564387605	1.396133714	17
GOBP_NATURAL_KILLER_CELL_ACTIVATION	0.004275828	0.687339373	0.407017919	0.459674377	1.326670042	84
GOBP_POSITIVE_REGULATION_OF_CIRCADIAN_RHYTHM	0.041497976	1	0.222056046	0.555885413	1.375101718	17
GOBP_RESPONSE_TO_DIETARY_EXCESS	0.010846554	0.883816287	0.380730401	0.528741455	1.400012916	29
GOBP_RHYTHMIC_BEHAVIOR	0.016371489	1	0.352487858	0.482279255	1.329943237	45
HP_ABNORMALITY_OF_THE_BRAINSTEM_WHITE_MATTER	0.024219908	1	0.352487858	0.591988633	1.435800129	15
MCCLUNG_COCAIN_REWARD_4WK	0.026973027	1	0.276500599	0.437576454	1.253250481	76
SIMBULAN_UV_RESPONSE_IMMORTALIZED_DN	0.010996159	0.883816287	0.380730401	0.530155847	1.414825892	31
TSAI_RESPONSE_TO_RADIATION_THERAPY	0.002536916	0.687339373	0.431707696	0.56437291	1.506140902	31

Table S8 Selected radiation-specific significant gene sets after GSEA, for hippocampus after six months of exposure to radiation.

<i>pathway</i>	<i>pval</i>	<i>fdr</i>	<i>log2err</i>	<i>ES</i>	<i>NES</i>	<i>size</i>
DAZARD_UV_RESPONSE_CLUSTER_G6	0.007846611	0.514946629	0.380730401	0.423817591	1.241462689	144
ENK_UV_RESPONSE_KERATINOCYTE_DN	0.000221058	0.142361542	0.518848078	0.399948108	1.210695732	468
GENTILE_RESPONSE_CLUSTER_D3	0.02718544	1	0.352487858	0.465746079	1.288429696	53
GENTILE_UV_HIGH_DOSE_DN	0.040959041	1	0.222056046	0.380334809	1.136862596	284
GENTILE_UV_HIGH_DOSE_UP	0.040160643	1	0.224966094	0.53220722	1.35525562	22
GENTILE_UV_RESPONSE_CLUSTER_D4	0.026885051	1	0.352487858	0.467645014	1.293682869	53
GOBP_CELLULAR_RESPONSE_TO_IONIZING_RADIATION	0.007996066	0.514946629	0.380730401	0.471657789	1.335865608	72
GOBP_CELLULAR_RESPONSE_TO_RADIATION	0.01787342	0.959206852	0.352487858	0.405047888	1.196492849	178
GOBP_ERAD_PATHWAY	0.002534382	0.441264322	0.431707696	0.460072383	1.330703841	107
GOBP_MIDBRAIN_DEVELOPMENT	0.037130842	1	0.321775918	0.434458291	1.241346715	87
GOBP_MYELOID_DENDRITIC_CELL_ACTIVATION	0.037	1	0.234392647	0.496545105	1.306505521	29
GOBP_UBIQUITIN_DEPENDENT_ERAD_PATHWAY	0.002127409	0.441264322	0.431707696	0.476432458	1.358182644	84
GOCC_RNA_POLYMERASE_II_HOLOENZYME	0.024975025	1	0.287857117	0.445101148	1.257470378	69
HP_ABNORMAL_BRAINSTEM_MORPHOLOGY	0.047952048	1	0.204294757	0.383341358	1.140753604	242
HP_ATROPHY_DEGENERATION_AFFECTING_THE_BRAINSTEM	0.022424032	1	0.352487858	0.537227255	1.391766378	25
HP_HYPOPLASIA_OF_THE_BRAINSTEM	0.004127107	0.441264322	0.407017919	0.47206717	1.341975646	77
SESTO_RESPONSE_TO_UV_CO	0.025683497	1	0.352487858	0.418812427	1.215027477	117
SMIRNOV_RESPONSE_TO_IR_2HR_UP	0.004498909	0.441264322	0.407017919	0.504621653	1.393231427	52